J. Micropalaeontology, 45, 219–257, 2026
https://doi.org/10.5194/jm-45-219-2026

Journal of Micropalaeontology
Open Access

Marine palynology of the Alano di Piave Bartonian–Priabonian Global Stratotype Section and Point, NE Italy

Alexander J. P. Houben[1], **Alina I. Iakovleva**[2], **Simone Galeotti**[3], **and Henk Brinkhuis**[4,5]

[1]Geological Survey of the Netherlands TNO, Princetonlaan 6, 3584 CB, Utrecht, the Netherlands
[2]Geological Institute, Russian Academy of Sciences, Pyzhevsky pereulok 7, Moscow, 119017, Russian Federation
[3]Dipartimento di Scienze Pure e Applicate, Università degli Studi di Urbino Carlo Bo, Campus Scientifico "E. Mattei", 61029 Urbino, Italy
[4]Department of Ocean Systems research (OCS), NIOZ Royal Netherlands Institute for Sea Research, PO Box 1790 AB Den Burg, the Netherlands
[5]Department of Earth Sciences, Marine Palynology and Paleoceanography, Laboratory of Palaeobotany and Palynology, Faculty of Geosciences, Utrecht University, Princetonlaan 8a, 3584 CB Utrecht, the Netherlands

Correspondence: Alexander J. P. Houben (alexander.houben@tno.nl)

Received: 17 October 2025 – Revised: 30 January 2026 – Accepted: 30 January 2026 – Published: 2 April 2026

Abstract. Further strengthening the multidisciplinary stratigraphic and paleo-environmental analysis of the Global Stratotype Section and Point (GSSP) Bartonian–Priabonian boundary of the Alano di Piave section (NE Italy), here, we present a data report of a highly resolved, quantitative marine palynological study emphasizing organic walled dinoflagellate cysts (dinocysts). The ensuing dataset is interpreted in an exploratory sense through empirical paleo-ecological grouping and spectral analysis.

The palynological assemblages are rich, diverse, and well-preserved, dominated by cosmopolitan, open marine dinocyst taxa, indicating a persistently distal, open marine depositional setting. Overall, the assemblages are remarkably stable, with no significant biotic reorganization recorded across the GSSP level. Evident paleo-environmental change is linked to the Middle Eocene Climatic Optimum (MECO) and its aftermath, where a sapropelic interval likely reflects a pluvial phase with enhanced runoff. Spectral analysis reveals that the influx of marginal marine dinocysts is strongly paced by the 400 kyr long eccentricity cycle. This suggests that orbital-scale climate changes, likely related to monsoonal intensity and runoff, controlled sediment transport from proximal settings. This data report includes the formal description of one new genus (*Bujakidinium* gen. nov.) and four new species (*Impagidinium gedlii* sp. nov., *Guersteinia châteauneufii* sp. nov., *Guersteinia*? *sluijsii* sp. nov., and *Bujakidinium umbellum* gen. et sp. nov.). In addition, we provide an extensive taxonomic list with annotations and 18 plates with illustrations of the new taxa. A total of 52 additional plates are available in the Supplement. This data report thus provides a robust palynological framework for the Bartonian–Priabonian GSSP and will be the backbone for ensuing, more detailed analyses.

Published by Copernicus Publications on behalf of The Micropalaeontological Society.

1 Introduction

Only quite recently did the International Committee on Stratigraphy (ICS) formalize and officially ratify the hemipelagic Alano di Piave section in NE Italy as the location of the Bartonian–Priabonian stage Global Boundary Stratotype Section and Point (GSSP, Agnini et al., 2011, 2014, 2021, Fig. 1). The boundary is placed at a level of 63.57 m and coincides with the base of a prominent crystal tuff layer, known as the *Tiziano* bed. Astronomical tuning and radio-isotopic techniques yielded absolute ages of 37.710 and 37.762 Ma, respectively, for the GSSP horizon (Galeotti et al., 2019). Among foraminifera, important associated biostratigraphic events include the successive extinctions of large acarininids and *Morozovelloides crassatus*. The GSSP is also characterized by the appearance of common *Cribrocentrum erbae* and the range top of the *Chiasmolithus grandis* (both coccolithophorids). Recent marine palynological studies show that, in terms of organic walled dinoflagellate cysts or "dinocysts", the first occurrence (FO) of *Oligokolpoma agniniae* (~ 8 m below the GSSP boundary) and the FO of *Reticulatosphaera actinocoronata* (~ 8 m above the GSSP boundary) may be taken as additional biostratigraphic indicators of the Bartonian–Priabonian boundary (Fig. 2; Iakovleva, 2025). Furthermore, the GSSP is calibrated against Chron C17n.2n. For more information, including, e.g., location details and lithostratigraphic descriptions, the reader is referred to Agnini et al. (2021).

In terms of paleogeography, the Alano section is located within the western fringe of the Belluno Basin, which is positioned to the east of a carbonate ramp area, termed the Lessini Shelf (Bosellini, 1989), and to the south of an early Alpine landmass (Bosellini, 1989; see Fig. 1). This relatively deep-water, hemipelagic setting now allows us to link existing marine palynological records from the classic Priabonian-type sections near Priabona on the eastern Lessini Shelf (e.g., Brinkhuis, 1994; Houben et al., 2012, Fig. 1) with the late-Eocene records from central Italy, including the GSSP location of the Eocene–Oligocene boundary (EOB) and the base Rupelian Stage at Massignano (e.g., Brinkhuis and Biffi, 1993, Fig. 1) and beyond. In addition, the Alano section also contains a record of the so-called Middle Eocene Climatic Optimum (MECO) interval (see Bohaty and Zachos, 2003). Several studies addressed this interval at Alano specifically (Luciani et al., 2010; Spofforth et al., 2010; Galazzo et al., 2013).

While the quantitative calcareous microfossil distribution of the section has been intensively studied (e.g., Agnini et al., 2011; Toffanin et al., 2011), no detailed quantitative analysis of either biosiliceous or organic walled biotic remains has been carried out so far. Iakovleva (2025) initiated a palynological analysis of the section, emphasizing dinocysts (Fig. 2), finding well-diversified palynological associations, suitable for further quantitative marine palynological analysis. The latter exercise could provide important

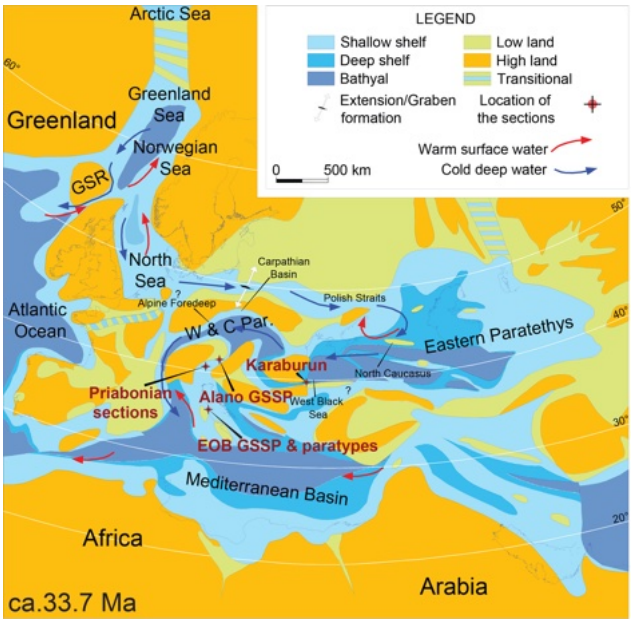

Figure 1. Map displaying the paleogeographic setting of the Alano section during Eocene–Oligocene boundary times (ca. 33.7 Ma). This figure serves specifically to address the context in the light of other Bartonian–Priabonian marine palynological reference sections. It illustrates a boreal-water influx in a dominant anti-estuarine circulation the Paratethys, extending into the Mediterranean Tethys. GSR: Greenland Scotland Ridge. W&C Par.: western and central Paratethys. The phrase "EOB GSSP and paratypes" refers to the Eocene–Oligocene boundary GSSP at Massignano and its paratypes. Adapted from Brinkhuis et al. (2025).

new complementary information regarding, e.g., the overall paleo-environmental setting and could potentially capture paleoceanographic and paleoclimatic changes across the Bartonian–Priabonian transition. Building on this foundation, we undertook a collective effort to generate a comprehensive marine palynological dataset to complement the existing micropaleontological and geochemical studies. In addition, we performed spectral analysis on the resulting dataset, calibrated against earlier studies (e.g., Galeotti et al., 2019) of the Alano GSSP. While emphasizing the distribution trends of dinocysts, we also include broad categories of other major aquatic algal categories, as well as sporomorph groups, providing a broad paleo-environmental land–sea assessment during the Bartonian–Priabonian transition across the nearby slope, shelf, and hinterland. We encountered four previously undescribed species and one new genus, not yet covered in Iakovleva (2025). These are formally described and depicted in the taxonomic section. In addition, we include many illustrations of the encountered dinocyst taxa in the Supplement (Plates S1–S52).

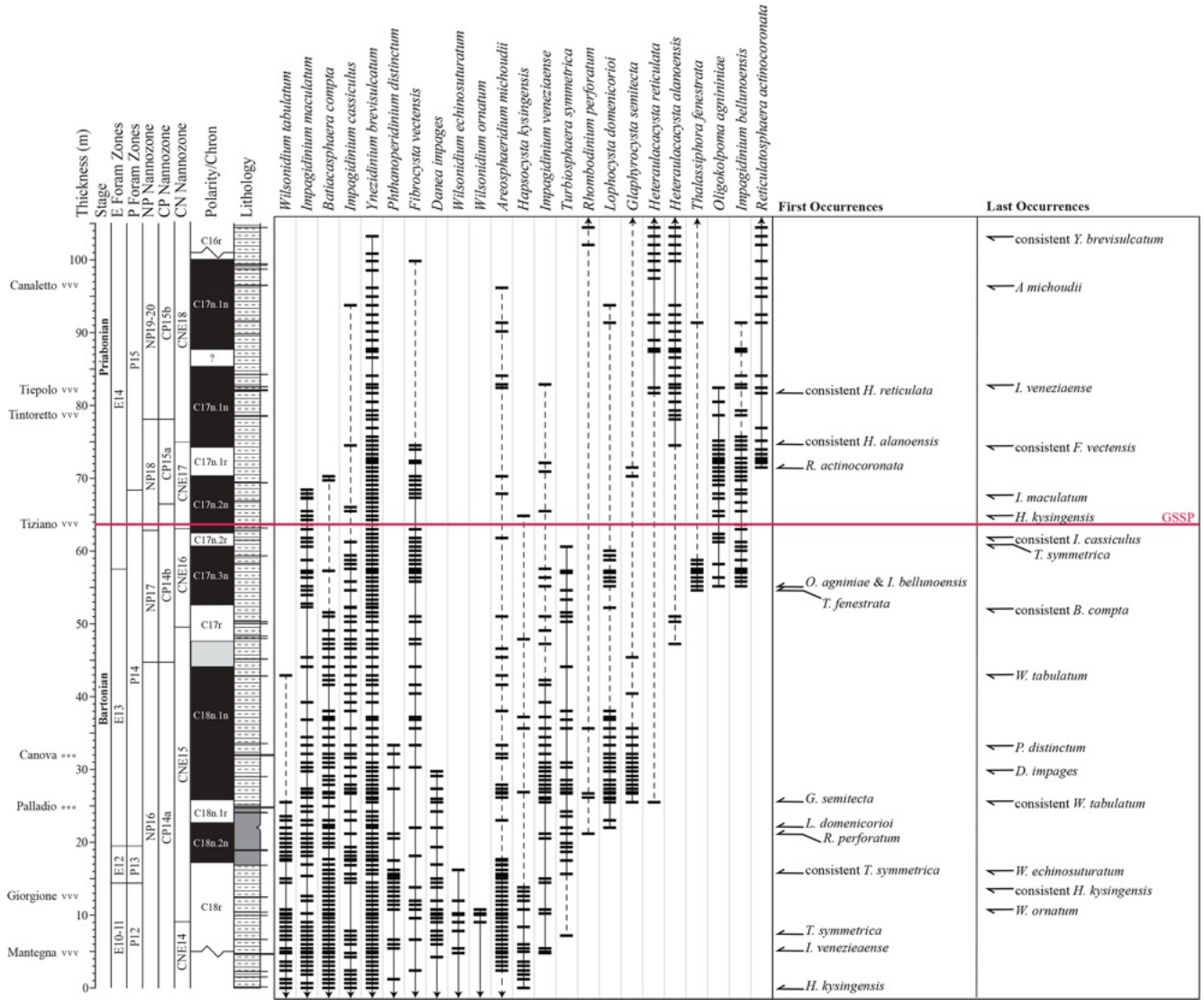

Figure 2. Schematic log, stratigraphic context, and important dinocyst index events after Iakovleva (2025). Volcanoclastic and bioclastic marker beds are indicated on the left side. The horizontal red line indicates the position of the GSSP.

2 Material and methods

The Alano di Piave section (45°54′51.10″ N, 11°55′4.87″ E) is located along the southern margin of the southern Alps, in the south of Belluno Province, NE Italy (Fig. 1). Geologically, this area belongs to the Belluno Basin, a paleogeographic domain formed in Jurassic times by the regional rifting that eventually led to the break-up and consequent collapse of predominantly Triassic shallow-water carbonate platforms (Winterer and Bosellini, 1981; see Fig. 1). Hemipelagic sedimentation persisted until the late Eocene. The ∼ 105 m thick section represents bathyal, offshore marine deposits, composed of grayish hemipelagic marls with intercalations of millimeter-thick sandy–silty layers, six crystal tuff layers, and two biocalcarenitic–ruditic beds (Agnini et al., 2011, 2021). Attempts to apply organic biomarker and Mg / Ca-based paleotemperature proxies have been unsuccessful. However, bulk-carbonate oxygen isotope data (Spofforth et al., 2010) reveal a stable equitable climate throughout Bartonian–Priabonian times. However, this is "interrupted" by the MECO episode (calibrated against the upper part of Chron C18r), which is terminated by a relatively abrupt cooling, associated with enhanced carbon burial during an interval calibrated to the lower portion of C18n.2n (Spofforth et al., 2010). Detailed sampling of the Alano GSSP section was coordinated and executed by the Agnini et al. (2011) team and was internationally distributed. Initial spectral analysis established a floating cyclochronology based on carbon isotope and wt % $CaCO_3$ records, calibrated against $^{206}Pb/^{238}U$ dating of zircons from four volcanic

tuffs. The resulting astrochronological and radio-isotopic estimates of the duration of intervals bracketed by consecutive crystal-rich volcanic tuff layers are in good overall agreement, but discrepancies of 40–160 kyr were noted (see Galeotti et al., 2019).

2.1 Palynological analysis

One hundred and fifty three samples, with an average spacing ca. 60 cm, were prepared at Utrecht University laboratories using standard palynological processing techniques described in, e.g., Cramwinckel et al. (2020). Identifiable (fragments of) palynomorphs were counted until a minimum of 200 identifiable dinocysts was reached. Other palynomorphs are assigned to seven broad categories, e.g., other remains of aquatic algae (mainly prasinophytes but also *Botryococcus*) including various acritarchs and (fragments of) benthic foraminiferal organic linings and terrestrial elements like bisaccate gymnosperm pollen, angiosperm pollen, and (fern, fungal) spores. The remaining material was scanned for rare dinocyst taxa. Dinocyst taxonomy follows that cited in Fensome et al. (2019), except for representatives of the subfamily of the Wetzelielloideae (see Bijl et al., 2017). For the analysis of marine palynological associations, emphasizing dinocysts, we rely on taxonomical and ecological dinocyst groups derived from modern distributions (e.g., Zonneveld et al., 2013; Marret and De Vernal, 2024) and empirically based paleo-ecological information or the Paleogene dinocysts following previous work (e.g., Brinkhuis, 1994; Pross and Brinkhuis, 2005; Sluijs et al., 2005; Frieling and Sluijs, 2018; Sluijs and Brinkhuis, 2024). Terrestrial and most aquatic palynomorphs are transported to the site of deposition. Consequently, a major transport distance bias can be expected based on differences in buoyancy and wind vs. water-based transport (e.g., Streel and Richelot, 1994; Abbink et al., 2004). This particularly pertains to bisaccate pollen, which is, therefore, considered to be a separate group. A detailed taxonomical section that describes selected new dinocyst taxa is included further below. All materials, including holotypes of new species, are stored in the collection of the Marine Paleoceanography and Palynology group (MPP), Laboratory of Palaeobotany and Palynology, Utrecht University, the Netherlands. All data are provided in the Supplement.

2.2 Spectral analysis

A multi-taper method (MTM) analysis has been conducted on various parameters derived from the quantitative palynological dataset. The MTM has been run with three tapers and a time-bandwidth product of 2 using the robust noise estimation algorithm of Mann and Lees (1996) to identify components exceeding the 95 % confidence level. Before running the analysis, all records were interpolated to a sampling rate of 60 cm and ere detrended by using a locally weighted scatterplot smoothing (LOWESS) with a window corresponding to 35 % of the total record length.

Spectral analysis has been conducted on two distinct intervals: from the base of the section to 40 m (from here onwards "the lower segment") and from 35 m to the top of the section (from here onwards "the upper segment"). The lower segment is characterized by larger fluctuations in the $\partial^{13}C$ and $CaCO_3$ records (Spofforth et al., 2010) and in the palynological associations, across the interval corresponding to the Middle Eocene Climatic Optimum (MECO). For the lower interval, the MTM analysis has been conducted in the depth domain. For the upper interval, we use the floating cyclochronology of Galeotti et al. (2019) to transfer the analyzed records in the time domain before running the MTM analysis.

Considering an average sedimentation rate of $\sim 3\,cm\,kyr^{-1}$ (Galeotti et al., 2019), the sampling rate of 60 cm corresponds to ~ 20 kyr in the time domain, which does not permit the detection of higher-frequency astronomical forcing components (precession and obliquity) but is sufficient to detect the short and long eccentricity components. Based on a total duration of 1.675 Myr for C18n for the 29 m thick C18n, the lower segment is deposited at a sedimentation rate of $\sim 1.75\,cm\,kyr^{-1}$. Hence, the sampling rate in the time domain is ~ 35 kyr across this interval, which is only sufficient to detect the long eccentricity component.

3 Results

3.1 Palynology

Most samples reveal rich and reasonably preserved palynodebris and palynomorph (combined termed "palynofacies") associations. The palynodebris is typically of a mixed nature, with, e.g., various contributions of transparent to pale-brown-colored discrete to fluffy amorphous elements alongside a suite of terrestrially derived plant materials (cuticles, tracheid material, resin, and leaf tissues) and opaque particles. No obvious trends are apparent from our semi-quantitative assessments (see Table S1 and the .xlsx file in the Supplement). An exception is the sapropelic interval above the MECO, where a consistently higher proportion of amorphous organic matter is noted. In samples with abundant prasinophyte algal cysts, these typically occur in a highly fragmented fashion; complete, isolated specimens are rather rare, causing issues with absolute quantification. These "absolute numbers" (and consequent percentages) should therefore be taken with caution and may thus not be accurately represented.

Strong shifts in the absolute (Fig. 3) and relative (Fig. 4) contributions of the different broad categories of palynomorphs are very limited throughout. On the other hand, trends in absolute palynomorph abundance are somewhat variable, lying between 2500 to 10 000 per gram. A conspicuous spike in concentration is recorded at the base of the sapropelic unit just above the MECO interval. The dinocyst

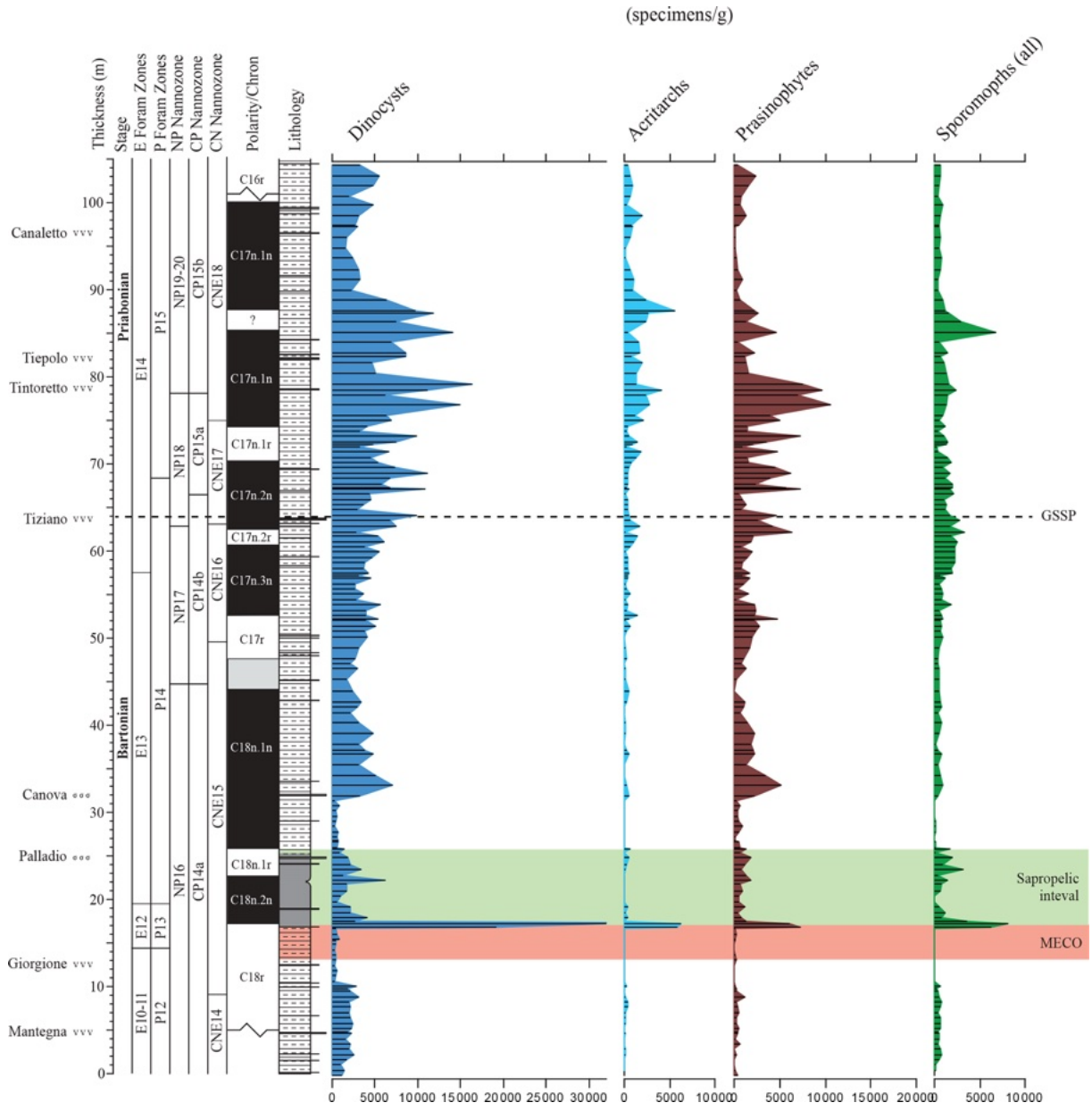

Figure 3. Weight-averaged concentration of palynomorph categories. The red shading marks the MECO interval as defined by a trend towards more negative $\partial^{18}O$ values (Spofforth et al., 2010). The green interval is the recovery of the MECO, which is accompanied by elevated total organic carbon (TOC) levels and sapropelic sedimentation. The GSSP level is indicated by a dotted horizontal line.

assemblages are taxonomically diverse (~ 100 taxa recognized; see Table S1 and the .xlsx file) and largely cosmopolitan in terms of their biogeographic affinity (see also Iakovleva, 2025). The category "prasinophyte algae" is mainly composed of *Schizosporis* spp. sensu Brinkhuis and Biffi (1993) and morphologically similar "pterospermel-lid" organic remains of unknown biological affinity (see, e.g., Plate S50, figs. 1–2, 3, 6, 9, and 12 and Plate S51, fig. 1 in the Supplement). Their conspicuous abundance in Bartonian to early-Priabonian times was noted earlier, e.g., in central and eastern Mediterranean and Peri-Tethyan sections (e.g., Brinkhuis and Biffi, 1993; Iakovleva et al., 2019; Iakovleva et al., 2020, 2024) but apparently also extended into the Atlantic domain, as reported by, e.g., Van Mourik et al. (2001) for Blake Nose, Bahama Bank. A better assessment of this group is yet to be conducted. The co-occurring sporomorphs are reasonably diversified but – perhaps not surprisingly, given the overall offshore environment – are consistently dominated by bisaccate pollen derived from gymnosperms. It may be noted, however, that studies from the younger

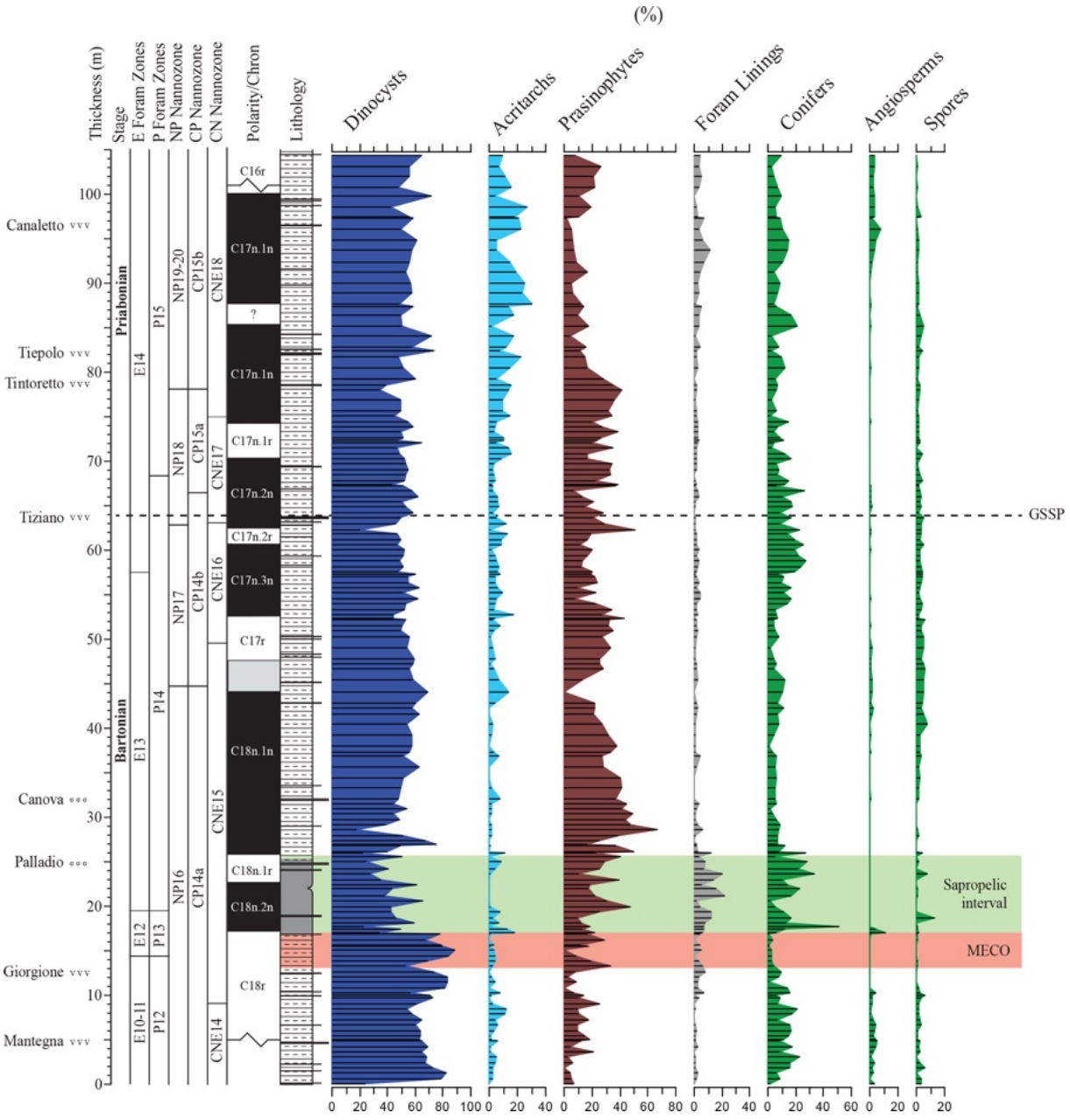

Figure 4. Relative abundance distribution of categories of the palynological associations.

portion of the Priabonian in the region show even higher concentrations and overwhelming dominance of the latter, a phenomenon linked to progressive climatic cooling across the Eocene–Oligocene Transition (EOT) (e.g., Brinkhuis and Biffi, 1993; Brinkhuis, 1994; Houben et al., 2012; Kaya et al., 2025).

For the purpose of the present paper but also out of practical needs (identification and counting consistency between the authors), we opted to create several morphological "complexes" (cpx) of morphologically closely related taxa. These are summarized in Table 1 and further discussed in Sect. 3.2, and the annotated species list is in Appendix B.

The dinocyst assemblages (Fig. 5) contain but few peridinioids. Among the gonyaulacoids, the dominant category is the open marine *Spiniferites ramosus* complex. Among the most offshore taxa, representatives of *Nematopshaeropsis* are constantly present, while those assigned to the *Impagidinium* cpx are common. Members of the Goniodomids and representatives of *Operculodinium* and *Enneadocysta* cpx are also quite common. The MECO also does not stand out in terms of changes in dinocyst assemblage composition (Figs. 4 and

Table 1. Composition of morphological groups and complexes.

Group	Included taxa
Deflandrea	*Deflandrea, Palaeocystodinium, Senegalinium*
Goniodomids	*Bujakidinium, Eocladopyxis, Heteraulacacysta, Homotryblium, Polysphaeridium*
Wetzelielloids	*Charlesdowniea, Rhombodinium, Wetzeliella, Wilsonidium*
Areoligeraceans	*Glaphyrocysta*
Cleistosphaeridium cpx	*Adnatosphaeridium, Batiacasphaera, Cleistosphaeridium, Dapsilidinium, Diphyes, Distatodinium, Elytrocysta, Hystrichokolpoma, Oligokolpoma*
Cribroperidinium-Cordosphaeridium cpx	*Achilleodinium, Cordosphaeridium, Cribroperidinium, Damassadinium, Fibrocysta, Pentadinium, Samlandia, Turbiosphaera*
Enneadocysta-Areosphaeridium cpx	*Areosphaeridium, Cooksonidium* group*, *Enneadocysta, Stoveracysta*
Protoperidinioid cysts	*Lejeunecysta, Selenopemphix*
Cerebrocysta cpx	*Cerebrocysta, Corrudinium, Pyxidinopsis*
Spiniferites ramosus cpx	*Achomosphaera, Hystrichostrolgylon, Melitasphaeridium, Reticulatosphaera, Rottnestia, Spiniferella, Spiniferites*
Impagidinium cpx	*Guersteinia, Hapsocysta, Impagidinium, Ynezidinium*

* Contains the morphologically continuous genera *Cooksonidium, Hemiplacophora*, and *Schematophora*.

5). The post-MECO sapropelic interval contains high but fluctuating amounts of sporomorphs (up to 50 %), prasinophytes (up to 40 %), and organic foraminiferal linings (up to 20 %), while dinocysts decrease from 80 % to 30 % immediately above the end of the MECO (Fig. 4). Remarkably, a distinct rise in *Spiniferites pseudofurcatus* (up to 70 %), correlating to a strong decrease in prasinophyte remains, is recorded within the middle part of this interval.

3.2 Paleo-environmental assessment

For paleo-environmental interpretations, the morphological dinocyst complexes are assigned to four morphology-based "eco-categories" sensu, e.g., Brinkhuis (1994), Pross and Brinkhuis (2005), and Frieling and Sluijs (2018), viz those thought to represent (1) restricted marine settings (representatives of Goniodomids with an epicystal archaeopyle, *Phthanoperidinium*, and *Deflandrea* spp.); (2) marginal marine and inner neritic settings (e.g., all wetzelielloids, areoligeraceans, *Cleistosphaeridium* cpx, *Cribroperidinium/Cordosphaeridium* cpx, *Enneadocysta/Areosphaeridium* cpx, *Spiniferites pseudofurcatus*, and *Thalassiphora* spp.); (3) outer neritic settings (Protoperidinioid cysts, *Operculodinium* spp., *Cerebrocysta* cpx, and the *Spiniferites ramosus* cpx); and (4) typically offshore, oceanic settings (*Impagidinium* cpx and *Nematosphaeropsis* spp.). Note that some taxa were left out of these proximal–distal considerations (e.g., *Lingulodinium* spp.) because their paleo-ecological range is considered to be highly variable and non-specific. A summation of all of the relative abundance distributions of these four eco-categories, together with relevant geochemical information, is shown in Fig. 6. Note that these groups were subsequently included in the spectral analysis exercise, discussed further below. Purely based upon visual inspection, one may note a persistent dominance of outer neritic and oceanic taxa, which, together, often exceed 90 % of the assemblage. Noteworthy features are (1) the relative increase in the oceanic and outer neritic group over the course of MECO warming, (2) the pulse-like dominant incursions of marginal marine and restricted taxa in association with the sapropelic level above MECO (Chron C18n), and (3) a gentle increase in restricted marine taxa in the early Priabonian. Above the *Tiepolo* ash horizon (82 m up-section height, C17n.1n), relative abundances reach 40 %. Other than these trends, no major shifts or clear cyclic pacing are evident (Fig. 6).

3.3 Spectral analysis

The spectral analysis involved the analysis of broad palynological categories or "parameters" (e.g., sporomorphs, dinocysts, acritarchs, prasinophytes, percentages, and specimens per gram) and the more specific eco-groups of dinocysts, as defined above.

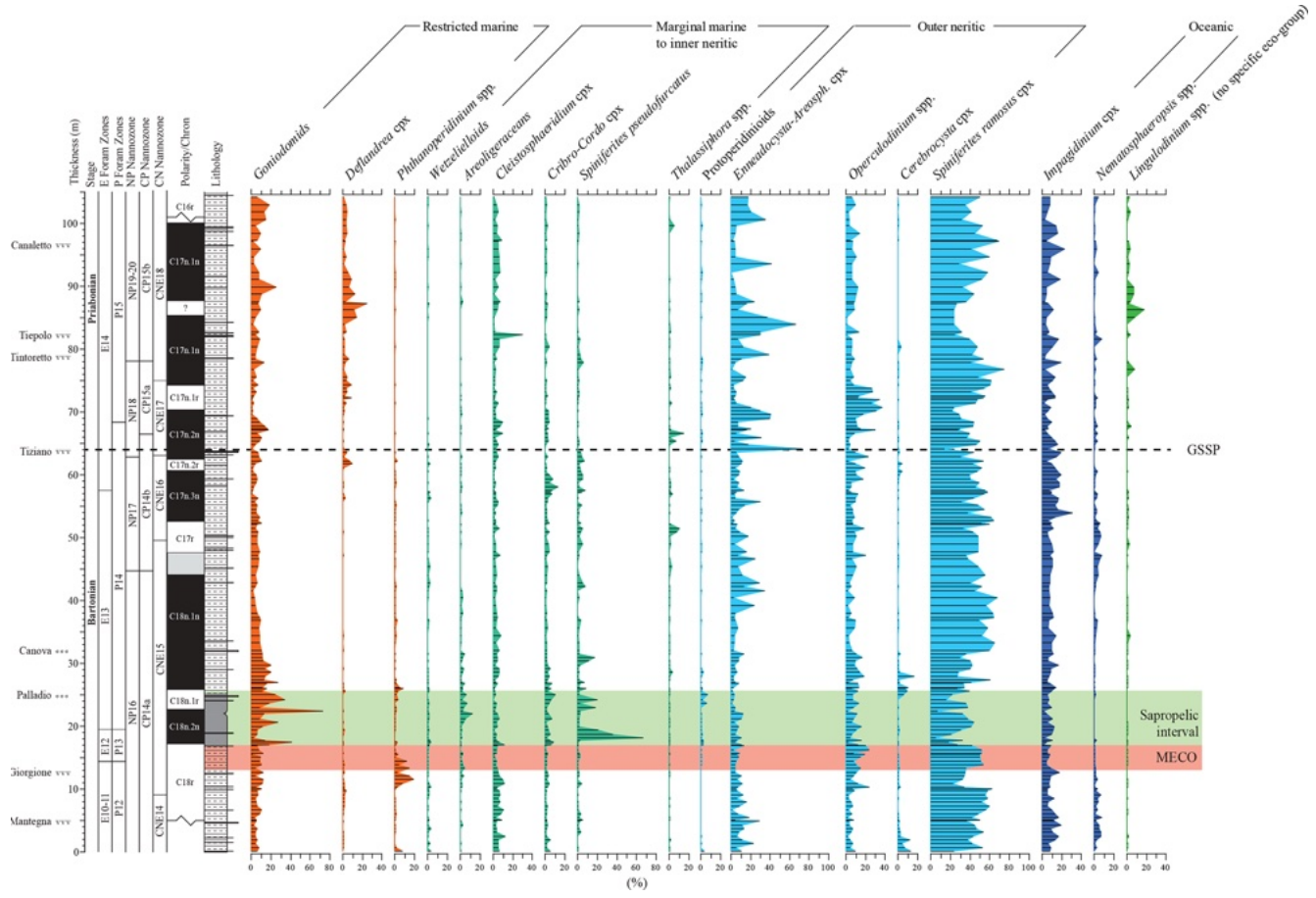

Figure 5. Relative abundance of selected dinocyst taxa and complexes (Table 1). Taxa are plotted along an idealized proximal-to-distal marine transect; viz. from restricted marine to oceanic. *Lingulodinium* spp. is not included in this transect due to its mixotrophic physiology and broad ecological range. It is therefore plotted separately on the right side of the figure.

3.3.1 Lower segment (0–40 m)

Spectral analysis of the better-resolved wt % $CaCO_3$ and $\delta^{13}C$ records reveals rather different results (Fig. 7). The former is dominated by a peak of spectral density centered at ~ 0.14 cycles m^{-1}, corresponding to a wavelength of ~ 715 cm that can be interpreted to reflect the 405 kyr eccentricity based on sedimentation rate values. The absence of a short eccentricity component in the MTM spectrum indicates a markedly nonlinear response of the sedimentary system to astronomical forcing.

A peak exceeding the 99 % confidence limit is also present in the frequency range of obliquity. The sampling rate does not allow us to check for the presence of a precession component in the record as the corresponding frequency exceeds the Nyquist frequency. Remarkably, the MTM spectrum of $\delta^{13}C$ does not show a high spectral density at any frequency expected for astronomical forcing components. We interpret the lack of a clear astronomical forcing signature to result from the local features of the record that, just above the MECO, is dominated by the presence of an extended interval of black shale that is responsible for much of the total variance, possibly masking global features in the carbon isotope record of the lower segment at Alano di Piave.

We use the filter of the 405 kyr component of the wt % $CaCO_3$ to transfer the records of selected palynological parameters, including the number of dinocysts per gram of sediment and the relative abundance of prasinophytes and marginal marine dinocysts, into the time domain. No significant components referable to astronomical forcing are present in the MTM spectrum of the dinocyst per gram record (Fig. 8a). However, the MTM analysis of the relative abundance of prasinophytes and marginal marine dinocysts reveals high spectral density in the frequency range of the 405 kyr eccentricity, indicating a strong control of astronomical forcing on these two parameters.

3.3.2 Upper segment (35 m and higher)

The floating cyclochronology of the upper segment, available from Galeotti et al. (2019), allows us to transfer the records into the time domain. The results of the MTM anal-

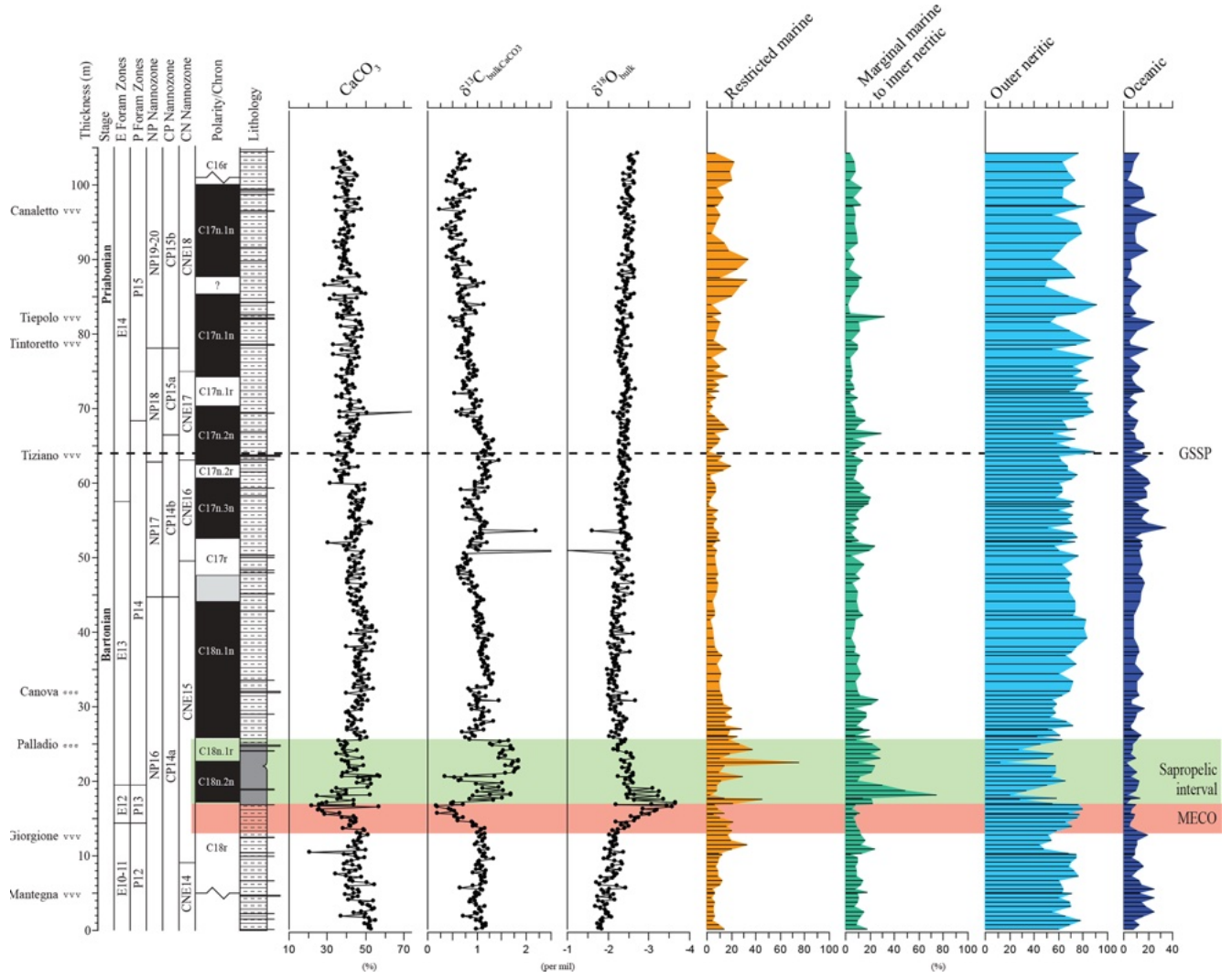

Figure 6. Relative abundance of the dinocyst-based ecological groups, ordered from proximal to the left to distal to the right. The data are complemented by carbonate weight percentage, ∂^{13}C bulk carbonate, and ∂^{18}O bulk carbonate after Spofforth et al. (2010) and Galeotti et al. (2019).

ysis carried out in the time domain are provided in Fig. 8b. Obtained results do not differ much from the results of the observation carried out on the lower segment, although the resolution in the domain is almost double. In particular, the relative abundance of shallow-water dinocysts is clearly controlled by long eccentricity. A relatively high spectral density (exceeding the 95 %) is also observed in the frequency range of short eccentricity. The relative abundance of the remains of prasinophytes shows a similar spectrum, although the 400 kyr component is not as clearly expressed as in the record of marginal marine dinocysts. Interestingly, the spectral analysis of this palynological category also shows high spectral density (exceeding the 99 % confidence limit) at the frequency of 0.058 cycles kyr^{-1}, which corresponds to a period of 173 kyr, similar to a modulation term of obliquity. However, considering the low resolution of our record, we cannot exclude the fact that this component results from an aliasing of precession.

The number of dinocysts per gram shows a high spectral density, exceeding the 95 % confidence limit, in the frequency range expected for short eccentricity. The 400 kyr eccentricity forcing also dominates the ∂^{13}C record (Galeotti et al., 2019), in line with observations from global records in the Paleogene (Westerhold et al., 2020).

Importantly, the well-expressed long eccentricity found to dominate the distribution of shallow-water dinocysts permits us to define the phasing relationship with the carbon isotope record. Filtering of this component from the carbon isotope record and from the record of the restricted and marginal marine dinocyst proportion reveals a clear antiphase relationship between the two signals (Fig. 9).

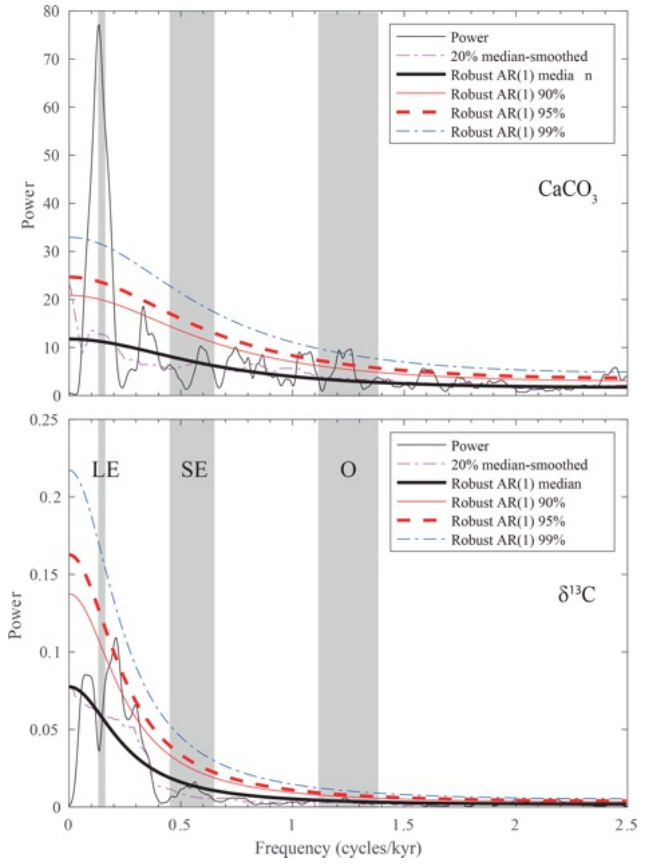

Figure 7. MTM spectra of the wt % $CaCO_3$ and $\delta^{13}C$ records from the lower segment of the Alano di Piave succession, carried out in the time domain. Vertical bands represent the expected frequency of long eccentricity (LE), short eccentricity (SE), and obliquity (O) based on sedimentation rate.

4 Concluding remarks

By presenting quantitative palynological and dinocyst data specifically, this data report complements other (semi-)quantitative palynological datasets from the greater central and eastern Para-Tethyan realm (e.g., Brinkhuis and Biffi, 1993; Brinkhuis, 1994; Houben et al., 2012; Bati, 2015; Iakovleva et al., 2019; Iakovleva et al., 2020; Sancay and Bati, 2020; Vasiliyeva and Musatov, 2023; Iakovleva et al., 2024: Kaya et al., 2025), extending it into the relatively deep-water setting of the Alano di Piave GSSP section.

A first observation is that in neither of the discussed groups or categories is an evident shift, change, or biotic reorganization recorded in association with the GSSP level. Overall, with the exception of the MECO and its aftermath, associations and assemblages are remarkably stable. The persistent presence of oceanic dinocyst groups (Fig. 6) indicates continuous deposition in a distal, continuously open marine, hemipelagic setting. The introduction of more proximal marine dinocysts and sporomorphs is thought to be caused by transport from adjacent, relatively nearby shallow-water platforms, e.g., from the Lessini Shelf (Priabonian-type area). The spectral analysis results show that transport from proximal settings is – on the investigated temporal scale – modulated by long-eccentricity cyclicity. Through modulating precession and, therefore, monsoonal intensity, a link with rhythmic changes in run-off can be envisaged, and changes in eustatic sea level are not necessarily involved.

This compositional stability is in accordance with the offshore, bathyal, hemipelagic position of Alano di Piave (e.g., Agnini et al., 2011). In addition, it also illustrates the profound climatic stability throughout Bartonian and early-Priabonian times, with the exception of the MECO and its aftermath. Such stability can also be deduced from paleotemperature and oxygen isotopic data from the Bartonian and early-Priabonian interval (see e.g., Zachos et al., 2008; Bohaty et al., 2009; Houben et al., 2019; Westerhold et al., 2020). This stability preceded cooling and subsequent glacial expansion across the EOT, starting at a correlative level within Chron C13r (e.g., Wade et al., 2012 and Haiblen et al., 2019; Kaya et al., 2025).

The MECO is associated with a progressive decrease in restricted and marginal marine dinocyst taxa (Figs. 5 and 6). This may reflect a subtle record of a transgressive and/or retrogradational (condensed) sequence. Clear shifts in the palynological associations do occur in the sapropelic levels above the MECO. This interval is accompanied by an increase in terrigenous palynomorphs and in typical restricted marine to coastal dinoflagellates. Since a coeval increase in dinocysts typical for eutrophic, high nutrient conditions (e.g., (proto)peridinioids, *Lingulodinium* spp.) is absent, it appears to be the case that the sapropelic interval is not related to strong eutrophication. Instead, we surmise that the sapropelic interval above and/or after MECO reflects an interval of strong surface water stratification and poor ventilation, perhaps associated with a pluvial phase, somewhat analogously to mechanisms suggested for the mid-Cretaceous Oceanic Anoxic Events (e.g., Jenkyns, 2010), in turn related to enhanced hydrological cycling brought about by MECO warming.

This data report is accompanied by an extensive annotated species list (Appendix B) and numerous illustrative plates (Appendix C). Four new species and one new genus are formally described in the taxonomy section below. These complement the stratigraphically significant taxa that were described earlier by Iakovleva (2025) from the Alano section. This detailed taxonomic component of this data report will facilitate future detailed correlations and paleoenvironmental reconstructions of the Bartonian–Priabonian interval, within and beyond the (Para-)Tethyan realm.

Appendix A: Systematic paleontology

Division DINOFLAGELLATA (Bütschli, 1885); Fensome et al., 1993

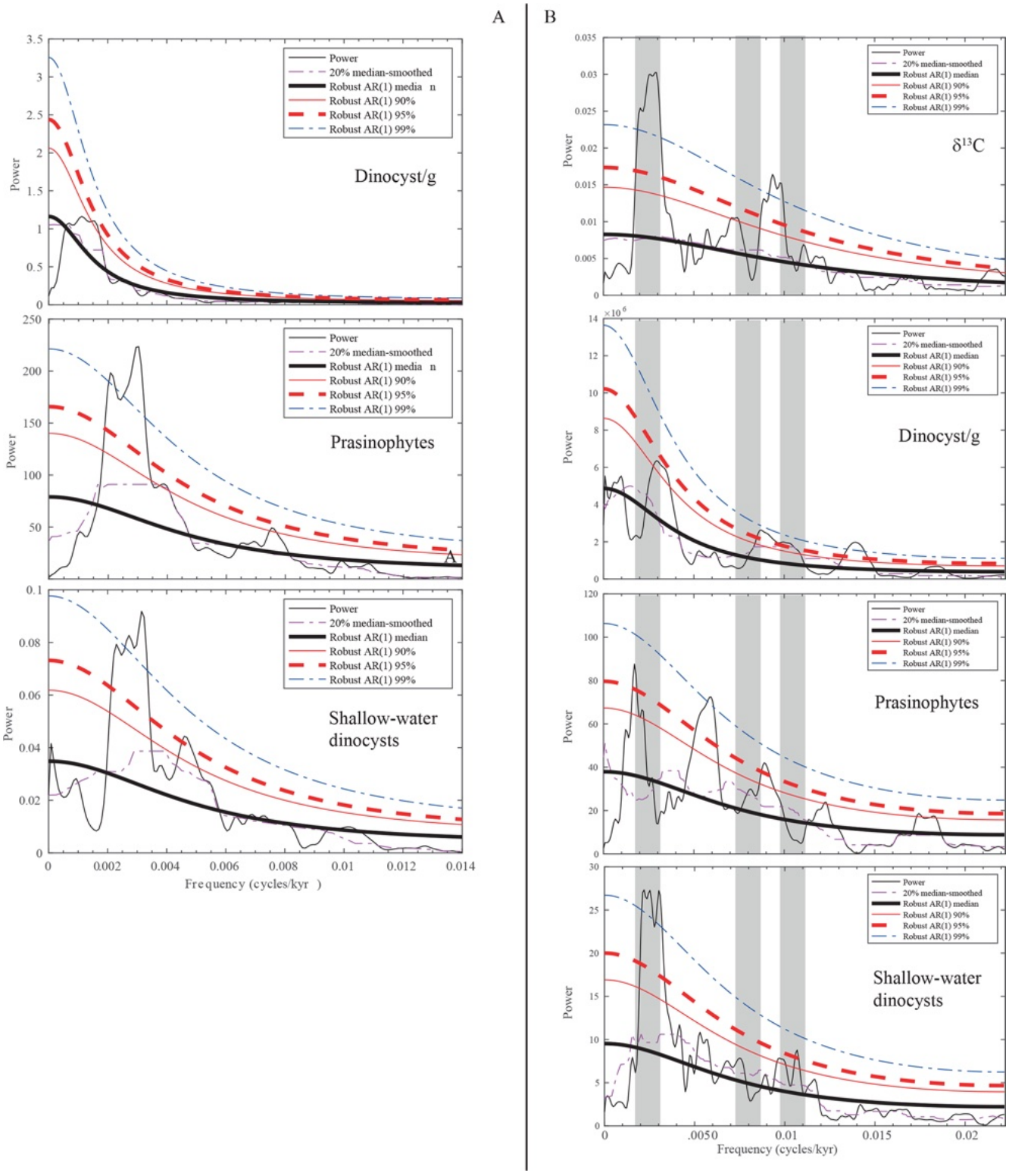

Figure 8. MTM spectra of selected palynomorph groups in the time domain: **(A)** for the lower segment and **(B)** for the upper segment.

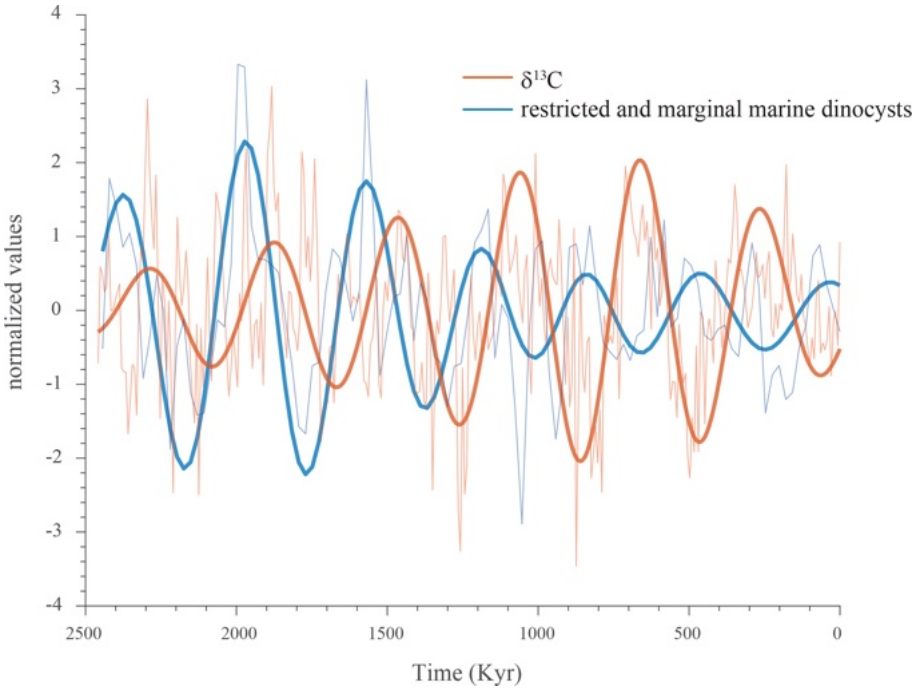

Figure 9. The 405 kyr component filtered from the $\partial^{13}C$ record (orange) and the summated proportions of restricted and marginal (shallow) marine dinocysts (blue), plotted against the normalized and detrended records.

Class DINOPHYCEAE Pascher, 1914

Subclass PERIDINIPHYCIDAE Fensome et al., 1993

Order GONYAULACALES Taylor, 1980

Suborder GONIODOMINEAE (Fensome et al., 1993)

Family GONIODOMACEAE (Lindemann, 1928)

Subfamily GONIODOMOIDEAE (autonym)

Genus ***Bujakidinium*** gen. nov.

Type *Bujakidinium umbellum* gen. et sp. nov. Plate C9 (figs. 2, 5, 8)

Derivation of name. In honor of Jonathan P. Bujak and in recognition of his achievements in palynology and biostratigraphy.

Diagnosis. Small to intermediate-sized, ovoidal to spherical proximochorate cysts bearing numerous intratabular, hollow processes, which are distally connected by an often perforated, thin ectophragm. Archaeopyle epicystal, combination archaeopyle, type (tAtP), operculum free.

Comparison. Bujakidinium gen. nov. clearly has morphological affinities with *Polysphaeridium* and, notably, *Hemicystodinium* (now synonymous with *Polysphaeridium*) but differs distinctly with regard to the possession of an ectophragm, leading to distally connected processes. In comparable current generic concepts, the presence or absence of an ectophragm is the basis upon which to distinguish between dinoflagellate cyst genera.

Bujakidinium umbellum gen. et sp. nov.: Pl. VI, figs. 8–12; Plate C9, figs. 1–10; Plate C11, figs. 3, 8, and 11.

Derivation of name. From the Latin *umbella* (umbrella), in reference to the presence of an ectophragm, represented by an often-perforated membrane.

Diagnosis. A species of *Bujakidinium* characterized by its intermediate size and thin, often perforated ectophragm.

Holotype. Plate C9 (2, 5, 8); sample A000, slide 2, EF: V30.

Paratype. Plate C9 (1, 4, 7, 10); sample A060, slide 2, EF: N22.

Type stratum and locality. Sample A000; level 0 m; Alano di Piave section, Italy.

Stratigraphic horizon. Bartonian–Priabonian.

Description.

Shape: subspherical to ovoidal.

Wall relationships: a smooth to scabrate endophragm and (appressed) periphragm, with the latter giving rise to numerous short hollow processes, distally connected by a thin, often perforated ectophragm.

Wall features: the endophragm and periphragm are appressed between processes, and both are smooth to scabrate, while the ectophragm is thin and perforated.

Processes: smooth, hollow, narrow, and sometimes arranged in intratabular groups.

Paratabulation: gonyaulacacean, Goniodomid, indicated by archeopyle only.

Archeopyle: epicystal, type (tAtP), operculum free.

Size. Intermediate.

Dimensions. Holotype. Inner body: 51 × 49 µm; overall size: 72 × 73 µm. Mean values between 45 × 58 µm and 55 × 78 µm ($n = 10$).

Comparison. Bujakidinium umbellum has affinities with *Polysphaeridium congregatum* but clearly differs in having much thinner and longer processes and in that they are distally connected by a perforate membrane (ectophragm).

Suborder GONYAULACINEAE (autonym)

Family GONYAULACACEAE Lindemann, 1928

Subfamily GONYAULACOIDEAE Fensome et al., 1993

Genus ***Guersteinia*** Sluijs and Brinkhuis, 2024

Type Williams and Downie, 1966, pl. 26, fig. 8 as *Thalassiphora delicata*

Guersteinia châteauneufii sp. nov.: Plate C10, figs. 1–12; Plate C11, figs. 1–2, 4–7, 9–10, 12; Plate C13, figs. 1–3, 6–7.

Derivation of name. Named for Jean-Jacques Châteauneuf in recognition of his achievements in palynology, BRGM, Orlèans, France.

Diagnosis. Intermediate-sized representatives of *Guersteinia*, i.e., a thin-walled camocavate gonyaulacoid cyst with a subspherical central body and a moderately developed, smooth periphragm featuring faint traces of paratabulation and with cingular ridges with serrate to denticulate margins.

Holotype. Plate C10 (figs. 7–8, 10–11); sample A780, slide 1, EF: P22/2.

Paratype. Plate C10 (figs. 1–5); sample A3918, slide 1, EF: F34.

Type stratum and locality. Sample 780; level 7, 80 m; Alano di Piave section, Italy.

Stratigraphic horizon. Bartonian–Priabonian.

Description.

Shape: endophragm and periphragm are subspherical.

Wall relationships: cyst camocavate; endophragm and periphragm are appressed in the mid-dorsal area.

Wall features: endophragm and periphragm thin and smooth. The margins of periphragm are serrate. Faint features on the periphragm likely reflect paratabulation. Paracingulum indicated by low ridges, typically with denticulate to serrate margins.

Processes: absent.

Paratabulation: likely standard symmetric sexiform gonyaulacoid tabulation, indicated by periphragmal features of low relief, accompanied by low denticulate cingular ridges.

Paracingulum: indicated by parasutural features (low denticulate ridges) on the periphragm.

Parasulcus: indicated by parasutural ridges of low relief on the periphragm.

Archeopyle: precingular, type P (paraplate 3″), operculum free.

Size: intermediate.

Dimensions. Holotype. Inner body: 41 × 49 µm; overall size: 56 × 72 µm. Mean values between 39 × 55 µm and 51 × 75 µm ($n = 6$).

Comparison. Guersteinia châteauneufii differs from other species of *Guersteinia* due to having denticulate to serrate paracingular ridges and a relatively narrow pericoel.

Guersteinia?sluijsii sp. nov.: Plate C1, figs. 1–4; Plate C2, figs. 1–8; Plate C3, figs. 1–6; Plate C4, figs. 1–4; Plate C5. figs. 1–4; Plate C6, figs. 1–2, 5–6; Plate C7, figs. 1–6; Plate C8, figs. 1–6.

2004 *Aiora* sp. A, Gedl, 2004b: plate 8, figs. R and T–V.

Derivation of name. Named for Appy Sluijs in recognition of his achievements in marine palynology, organic biogeochemistry, paleoceanography, and paleoclimatology, Utrecht University, The Netherlands.

Diagnosis. Large to intermediate sized, likely representative of *Guersteinia*, i.e., a thin-walled camo (?) cavate gonyaulacoid cyst with a subspherical to elongated central body and a partly developed, smooth, large periphragmal distal "ring" supported by six to seven strands featuring potential traces of paratabulation. Archeopyle is unclear but likely precingular, operculum free.

Holotype. Plate C1 (figs. 1–4); sample A1260, slide 1, EF: F26/3.

Paratype. Plate C2 (figs. 1, 3, 6); sample A1260, slide 1, EF: H20.

Type stratum and locality. Sample 1260; level 12, 60 m; Alano di Piave section, Italy.

Stratigraphic horizon. Bartonian–Priabonian.

Description.

Shape: endophragm – subspherical to ellipsoidal; periphragm – partly developed, distally extended, ring shaped, typically characterized by six broad "strands" or processes expanding from the central body in distally curved, "aqueduct-shaped" terminations. One other type of extension is broader and wider than the others, almost sheet- or platform-like, with ridge-like features of low relief potentially indicating paratabulation, possibly a reflection of the

sulcal area. Also, the "strands" have low ridges along their length that may be taken to indicate parasutures.

Wall relationships: cyst likely camocavate, but the ventral and dorsal sides are difficult to identify. If the "platform-like" extension does indeed reflect the parasulcal area, it may be used to orient the cyst. The "strands" are developed from areas that may perhaps reflect plate junctions, but this is unclear.

Wall features: endophragm – small, ellipsoidal, thin, and smooth, often ripped and broken; the large-sized periphragmal "ring" – subspherical to ellipsoidal, typically supported by six strands or processes, terminating in a half-ring-shaped (or aqueduct-shaped) fashion with different-sized openings. A seventh "broad, flat outgrowth" or "platform" feature is described above.

Processes: other than the strands and "platform" described above, no obvious other features.

Paratabulation: unclear.

Archeopyle: unclear, likely 3″.

Dimensions. Holotype. Inner body: 21 × 26 µm; overall size: 84 × 87 µm. Mean values between 18 × 32 µm and 79 × 101 µm ($n = 12$).

Stratigraphic range. Bartonian–Priabonian in the type locality; late Priabonian (Poland, Gedl, 2004b); Bartonian–Priabonian (Armenia, Iakovleva et al., 2024).

Comparison. Guersteinia? *sluijsii* sp. nov. has apparent morphological affinities with "*Thalassiphora rota"* (perhaps also a candidate to be placed in *Guersteinia*) of Schiøler (2005). The latter differs due to having a larger number of strands (processes in Schiøler, 2005) and apparently having a clear archaeopyle, representing the loss of 3″. *T. rota* also appears to be much younger, with the records being indicative of a late-Oligocene to Early-Miocene age (see Schøler, 2005).

Guersteinia? *sluijsii* sp. nov. also differs from *Guersteinia lacunata* (Vieira et al., 2018) Sluijs and Brinkhuis 2024 by having a less developed, smooth periphragm, supported by the mentioned six to seven strands. *G. lacunata* also appears to have a somewhat "wrinkled" periphragm that is opposite to the smooth nature of *G.*? *sluijsii*.

The faint to clear periphragmal ridges on the exterior of *G.*? *sluijsii* are reminiscent of the presumed paratabulation reflected by *Guersteinia delicata* (see Sluijs and Brinkhuis, 2024), but a convincing, systematic pattern has yet to be discerned.

Remarks. This species is questionably attributed to the genus *Guersteinia* since the nature of the archeopyle remains unclear. The morphology of *Guersteinia*, including *G.*? *sluijsii* and allied forms, warrants further study.

Genus ***Impagidinium*** Stover and Evitt, 1978

Type Cookson and Eisenack, 1965
(Pl. 12, figs. 5–6, as *Leptodinium dispertitum*)

Impagidinium gedlii sp. nov.: Plate C8, figs. 7–10; Plate C9, figs. 11–13; Plate C11, figs. 13–15; Plate C12, figs. 1–20; Plate C13, figs. 4–5, 9–21.

1993 *Impagidinium* sp. of Brinkhuis and Biffi, 1993: pl. VII, fig. 3.

2005 *Impagidinium* sp. A, *Impagidinium* sp. B, and *Impagidinium* sp. C of Gedl, 2005: pl. 8, figs. 1–13.

Derivation of name. Named for Przemysław Gedl in recognition of his achievements in palynology, Institute of Geological Sciences, Kraków, Poland.

Diagnosis. A small- to intermediate-sized representative of *Impagidinium*, spherical to ellipsoidal in outline, with highly variable, typically convex to concave, smooth, low to intermediate–high parasutural septa with smooth or slightly denticulate distal margins.

Holotype. Plate C12 (figs. 1, 5, 9, 13); sample A240, slide 1, EF: V28.

Paratype 1. Plate C12 (figs. 2, 6, 10, 14); sample A1260, slide 1, EF: T18/2.

Paratype 2. Plate C12 (figs. 17–18); sample A10069, slide 2, EF: Q20.

Paratype 3. Plate C12 (figs. 15–16, 19–20); sample A240, slide 1, EF: M25/3.

Paratype 4. Plate C11 (figs. 13–15); sample A3030, slide 2, EF: Q33.

Paratype 5. Plate C13 (figs. 4–5, 9–13); sample A840, slide 1, EF: F27/3.

Type stratum and locality. Sample A240; level 2, 40 m; Alano di Piave section, Italy.

Stratigraphic horizon. Bartonian–Priabonian.

Description.

Shape: inner wall: spherical to ellipsoidal; outer wall: (septae) outline idem to cruciform.

Wall features: the smooth, thin-walled endophragm is overlain by a closely appressed, equally smooth periphragm, giving rise to smooth parasutural septa of highly variable but typically intermediate to high height; septae may distally be slightly microdenticulate or sometimes irregularly denticulate. Occasionally, septa may be concave in the precingular and postcingular areas. In extreme cases, the convex, high septa occur only in the apical, antapical, and cingular areas, almost with the development of short processes inside the sutural crests, while, in the precingular and postcingular areas, parasutural septa are almost invisible.

Processes: absent.

Paratabulation: indicated by parasutural features (septa); sexiform gonyaulacean, S-type sulcal arrangement typical for *Impagidinium*; formula 3′, 5–6″, 5c, 5‴, 1p, 1⁗.

Archaeopyle: precingular, type P (paraplate 3″), operculum free.

Dimensions. Holotype. Inner body: 33 × 36 µm; overall size: 52 × 53 µm. Mean values between 29 × 37 µm and 49 × 61 µm ($n = 13$).

Comparison. I. gedlii sp. nov. differs from *I. japonicum* by often having a more ovoid central body and smaller-sized, more pleated septa, often with denticulate distal margins of septa and sometimes with concave septa in the precingular and postcingular areas. *I. gedlii* sp. nov. has some affinities with *Impagidinium cristatum* but differs in most cases by generally having wider parasutural folds with slight or pronounced serrated edges, as far as we can surmise from the original description. At the same time, extreme concave to cruciform specimens of *I. gedlii* sp. nov. differ from *I. cristatum* by means of the development of septa only in apical, cingular, and antapical areas, almost showing the development of short processes (i.e., paratypes 4 and 5).

Stratigraphic range. Bartonian–Priabonian in the type locality; Bartonian (Armenia; Iakovleva et al., 2024); Priabonian (Uzbekistan; Iakovleva et al., 2019); Priabonian–early Oligocene (Poland; Gedl, 2004a, 2005); Ypresian–Priabonian (northern Caucasus; Iakovleva et al., 2020; Shcherbinina et al., 2020).

Remarks. The species appears to be very long ranging; it was noted in Ypresian assemblages recovered from Core RH-323 in the northern Negev Desert (southern Israel; see Fokkema et al., 2022) and in Priabonian–Rupelian materials from Italy and Türkiye (see Brinkhuis and Biffi, 1993; Brinkhuis, 1994; Kaya et al., 2025), but, so far, it has only been noted as being from low-latitude sites (all HB pers. obs.).

Appendix B: Annotated species list

Achilleodinium biformoides s.l.

Remarks. This group includes specimens found to be intermediate between *Achilleodinium biformoides* (Eisenack, 1954); Eaton, 1976 and types assignable to *Damassadinium crassimuratum* (Wilson, 1988); Fensome et al., 1993.

Achilleodinium? sp.

Remarks. This rare taxon is characterized by it relatively small size, its precingular archeopyle (reflecting 3"), and its fibrous periphragm, giving rise to intratabular process complexes with often small, tubular, distally closed sets of processes, with almost "hand-finger-shaped" terminations. In this sense, the species somewhat resembles the Late-Cretaceous–early-Paleogene *Florentina ferox*.

Achomosphaera alcicornu (Eisenack, 1954); Davey and Williams, 1966

Areosphaeridium diktyoplokum (Klumpp, 1953); Eaton, 1971

Areosphaeridium michoudii Bujak, 1994

Batiacasphaera compta Drugg, 1970

Bujakidinium umbrellum gen. et sp. nov. described herein

Cerebrocysta bartonensis s.l.

Remarks. This group includes *Cerebrocysta bartonensis* Bujak 1980 and other *Cerebrocysta* spp. which are not recognized at a specific level.

Charlesdowniea clathrata (Eisenack, 1938); Lentin and Vozzhennikova, 1989

Charlesdowniea clathrata subsp. *angulosa* (Châteauneuf and Gruas-Cavagnetto, 1978); Lentin and Vozzhennikova, 1989

Cooksonidium group

Remarks. In the Alano di Piave material, we recognized a suite of Areoligeracean taxa with mild dorso-ventral compression and variable intratabular and penitabular processes with end-members assignable to *Hemiplacophora semilunifera* Cookson and Eisenack, 1965; *Schematophora speciosa* (Deflandre and Cookson, 1955); Stover, 1975; and *Cooksonidium capricornum* (Cookson and Eisenack, 1965); Stover and Williams, 1995. This broad morphological variability (and similarity) came as a surprise to us and raises issues concerning the practical use of the employment of these forms (some of them placed in monospecific genera at this point) in regional and even global zonation schemes and age assessments (see Brinkhuis, 1992; Brinkhuis and Biffi, 1993; Bijl, 2022). Instead, our new data would suggest that the group needs serious taxonomic overhaul and that the individual morphologies cannot be used for precise age assessments.

Cordosphaeridium fibrospinosum group

Remarks. This group includes *C. cantharellus* (Brosius, 1963); Edwards, 2001; *C. exilimurum* (Davey and Williams, 1966); Fensome et al., 2009; *C. fibrospinosum* (Davey and Williams, 1966); Lentin and Williams, 1989; *C. gracile* (Eisenack, 1954); Lentin and Williams, 1985; *C. inodes* (Klumpp, 1953); Sarjeant, 1981; and *Muratodinium fibriatum* (Cookson and Eisenack, 1967); Drugg, 1970.

Corrudinium incompositum Wilson, 1988

Cribroperidinium spp.

Remarks. Specimens can mainly be assigned to either *Cribroperidinium tenuitabulatum* or *C. giuseppei*, pending the degree of paratabulation and growth bands reflected.

Danea impages (Damassa, 1979); Fensome et al., 1993

Deflandrea granulata Menéndez, 1965

Deflandrea heterophlycta Deflandre and Cookson, 1955

Deflandrea leptodermata Cookson and Eisenack, 1965

Deflandrea phosphoritica Eisenack, 1938

Diphyes colligerum (Deflandre and Cookson, 1955); Cookson, 1965

Distatodinium craterum Eaton, 1976

Distatodinium ellipticum (Cookson, 1965); Eaton, 1976

Enneadocysta spp.

Remarks. This group includes *Enneadocysta arcuata* (Eaton, 1971); Stover and Williams, 1995; *E. inessae* Iakovleva in Oreshkina et al., 2015; *E. multicornuta* (Eaton, 1971); Stover and Williams, 1995; *E. pectiniformis* (Gerlach, 1961); Stover and Williams, 1995; and *E. robusta* Stover and Williams, 1995.

Fibrocysta vectensis (Eaton, 1976); Stover and Evitt, 1978

Glaphyrocysta intricata (Eaton, 1971); Stover and Evitt, 1978

Glaphyrocysta microfenestrata (Bujak, 1976); Stover and Evitt, 1978

Glaphyrocysta semitecta (Bujak et al., 1980); Lentin and Williams, 1981

Guersteinia succincta (Morgenroth, 1966); Sluijs and Brinkhuis, 2024

Guersteinia chateauneufii sp. nov. described herein

Guersteinia? *sluijsii* sp. nov. described herein

Hapsocysta kysingensis Heilmann-Clausen and van Simaeys, 2005

Heteraulacacysta campanula Drugg and Loeblich, 1967

Heteraulacacysta alanoensis Iakovleva, 2025

Heteraulacacysta reticulata Iakovleva, 2025

Homotryblium aculeatum Williams, 1978

Homotryblium floripes (Deflandre and Cookson, 1955); Stover, 1975

Homotryblium tenuispinosum s.l.

Remarks. This group includes specimens with morphologies assignable to *H. tenuispinosum* Davey and Williams, 1966 and to *H. pallidum* Davey and Williams, 1966.

Homotryblium variabile Bujak et al., 1980

Hystrichokolpoma cinctum Klumpp, 1953

Hystrichokolpoma globulus Michoux, 1985

Hystrichokolpoma rigaudiae Deflandre and Cookson, 1955

Hystrichokolpoma salacia Eaton, 1976

Hystrichostrogylon membraniphorum Agelopoulos, 1964

Impagidinium aculeatum (Wall, 1967); Lentin and Williams, 1981

Impagidinium cassiculus Wilson, 1988.

Impagidinium dispertitum (Cookson and Eisenack, 1965); Stover and Evitt, 1978

Impagidinium gedlii sp. nov. described herein

Impagidinium maculatum (Cookson and Eisenack, 1961); Stover and Evitt, 1978

Impagidinium paradoxum s.l.

Remarks. Besides typical *I. paradoxum* (Wall, 1967); Stover and Evitt, 1978, we also encountered specimens with very high septa (Plate S46, figs. 3–4, 7), giving a "Christmas-star-like" appearance.

Impagidinium velorum s.l.

Remarks. This group includes specimens assignable to *I. velorum* Bujak, 1984 but is characterized in the Alano case by very high septa relative to a comparatively very small central body (see Plate S44, figs. 1–2, 4–5).

Impagidinium veneziaense Iakovleva, 2025

Impagidinium bellunoensis Iakovleva, 2025

Lingulodinium spp.

Remarks. This group includes *L. machaerophorum* (Deflandre and Cookson, 1955); Wall, 1967 and *L. strangulatum* (Rossignol, 1964); Islam, 1983.

Lophocysta domenicorioi Iakovleva, 2025

Melitasphaeridium pseudorecurvatum (Morgenroth, 1966); Bujak et al., 1980

Microdinium reticulatum group

Remarks. This group includes specimens assignable to *M. reticulatum* Vozzhennikova, 1967; *Histiocysta* spp.; and *Graptodinium* spp.

Minisphaeridium latirictum (Davey and Williams, 1966); Fensome et al., 2009

Nematosphaeropsis spp.

Oligokolpoma agnininiae Iakovleva, 2025

Operculodinium microtrianum (Klumpp, 1953); Islam, 1983

Operculodinium placitum Drugg and Loeblich, 1967

Operculodinium hirsutum (Ehrenberg, 1837); Lentin and Williams, 1973

Operculodinium nanaconulum Islam, 1983

Palaeocystodinium golzowense Alberti, 1961

Pentadinium goniferum Edwards, 1982

Pentadinium laticinctum Gerlach, 1961

Phthanoperidinium comatum (Morgenroth, 1966); Eisenack and Kjellström, 1971

Phthanoperidinium distinctum Bujak, 1994

Phthanoperidinium geminatum group.

Remarks. This group includes *P. geminatum* Bujak et al., 1980 and allied, morphologically related species like *P. clithridium, P. alectrolophum*, and *P. echinatum*.

Polysphaeridium spp.

Pyxidinopsis spp.

Reticulatosphaera actinocoronata (Benedek, 1972); Bujak and Matsuoka, 1986

Rhombodinium draco group.

Remarks. This group includes *R. draco* Gocht, 1955, *R. aidae* Iakovleva in Oreshkina et al., 2015, and *R. freienwaldense* (Gocht, 1955); Costa and Downie, 1979.

Rhombodinium perforatum (Jan du Chêne and Châteauneuf, 1975); Lentin and Williams, 1977

Rottnestia borussica (Eisenack, 1954); Eisenack, 1969

Samlandia chlamydophora Eisenack, 1954

Spiniferella cornuta (Gerlach, 1961); Stover and Hardenbol, 1994

Spiniferites pseudofurcatus (Klumpp, 1953); Sarjeant, 1981

Spiniferites rhomboideus Vieira and Mahdi, 2019

Spiniferites ristingensis Head, 2007

Stoveracysta spp.

Thalassiphora fenestrata Liengjarern et al., 1980

Thlassiphora gracilis Heilmann-Clausen and van Simaeys, 2005

Thalassiphora patula (Williams and Downie, 1966); Lentin and Williams, 1985

Thalassiphora pelagica (Eisenack, 1954); Eisenack and Gocht, 1960

Turbiosphaera symmetrica Bujak et al., 1980

Wetzeliella articulata Eisenack, 1938

Wetzeliella ovalis Eisenack, 1954

Wilsonidium echinosuturatum (Wilson, 1967)

Wilsonidium intermedium Cookson and Eisenack, 1961

Wilsonidium ornatum (Wilson, 1967); Lentin and Williams, 1976

Wilsonidium tabulatum (Wilson, 1967); Lentin and Williams, 1976

Ynezidinium brevisulcatum (Michoux, 1985); Lucas-Clark and Helenes, 2000

Appendix C

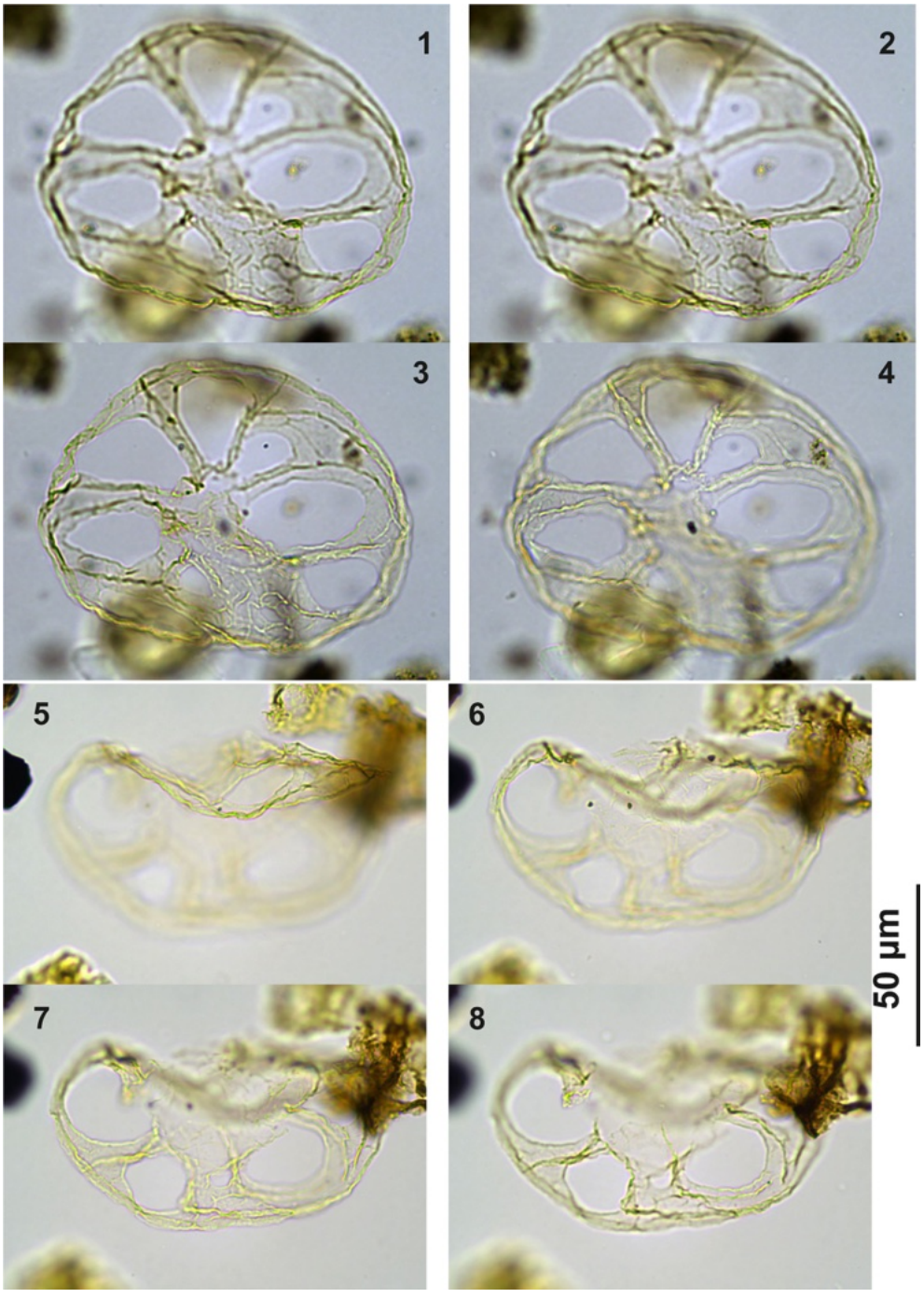

Plate C1. **(1–4)** *Guersteinia*? *sluijsii* sp. nov., holotype; sample A1260, slide 1, EF: F26/3. **(5–8)** *Guersteinia*? *sluijsii* sp. nov.; sample A5632, slide 1, EF: N18/3.

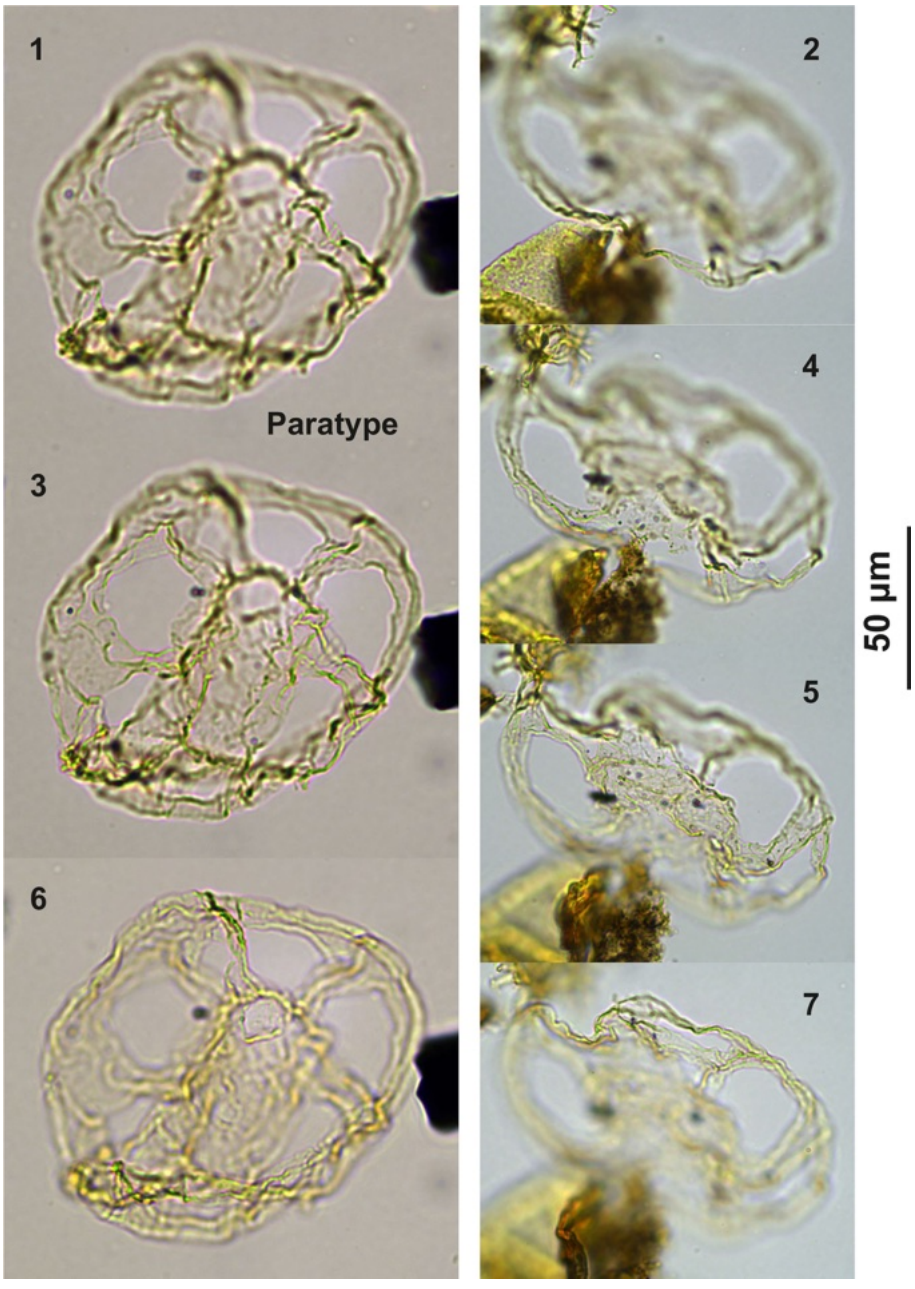

Plate C2. **(1, 3, 6)** *Guersteinia*? *sluijsii* sp. nov., paratype; sample A1260, slide 1, EF: H20. **(2, 4, 5, 7)** *Guersteinia*? *sluijsii* sp. nov.; sample A300, slide 2, EF: F17.

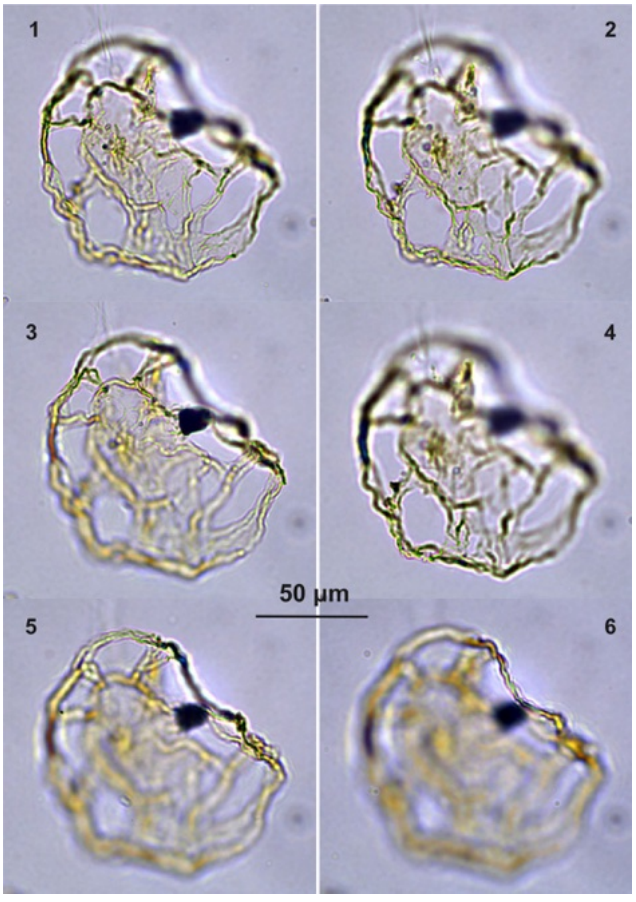

Plate C3. **(1–6)** *Guersteinia*? *sluijsii* sp. nov.; sample A5572, slide 1, EF: N17.

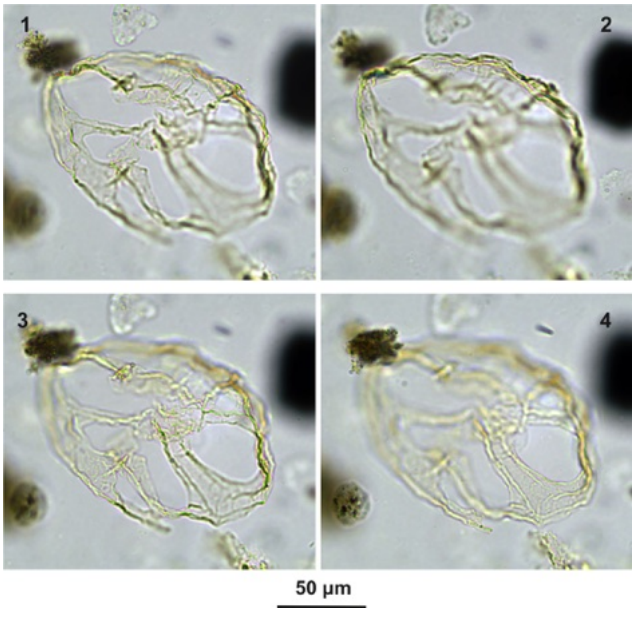

Plate C4. **(1–4)** *Guersteinia*? *sluijsii* sp. nov.; sample A4538, slide 1, EF: E31.

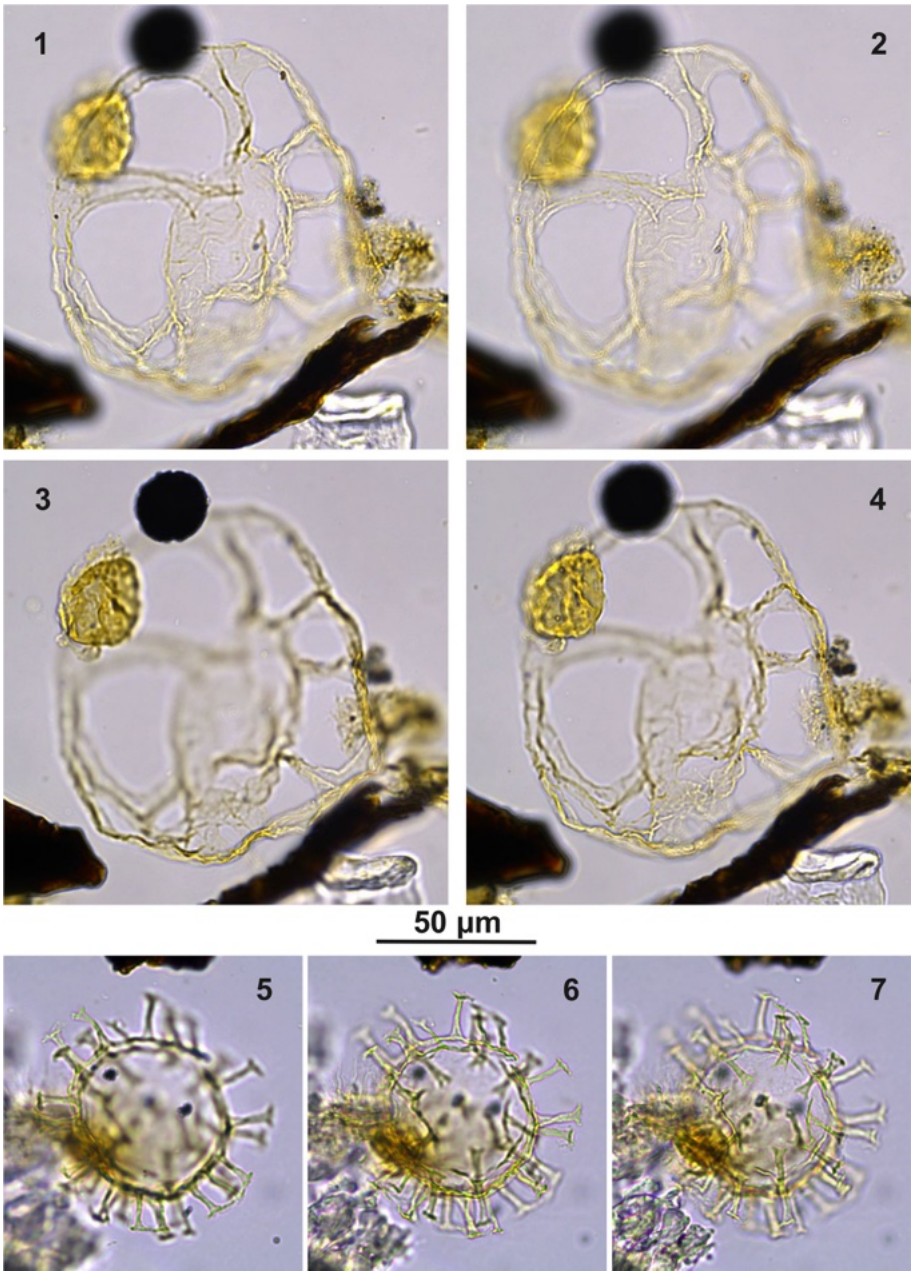

Plate C5. **(1–4)** *Guersteinia*? *sluijsii* sp. nov.; sample A5512, slide 2, EF: F28. **(5–7)** *Bujakidinium umbellum* gen. nov. sp. nov.; sample A5018, slide 2, EF: H22.

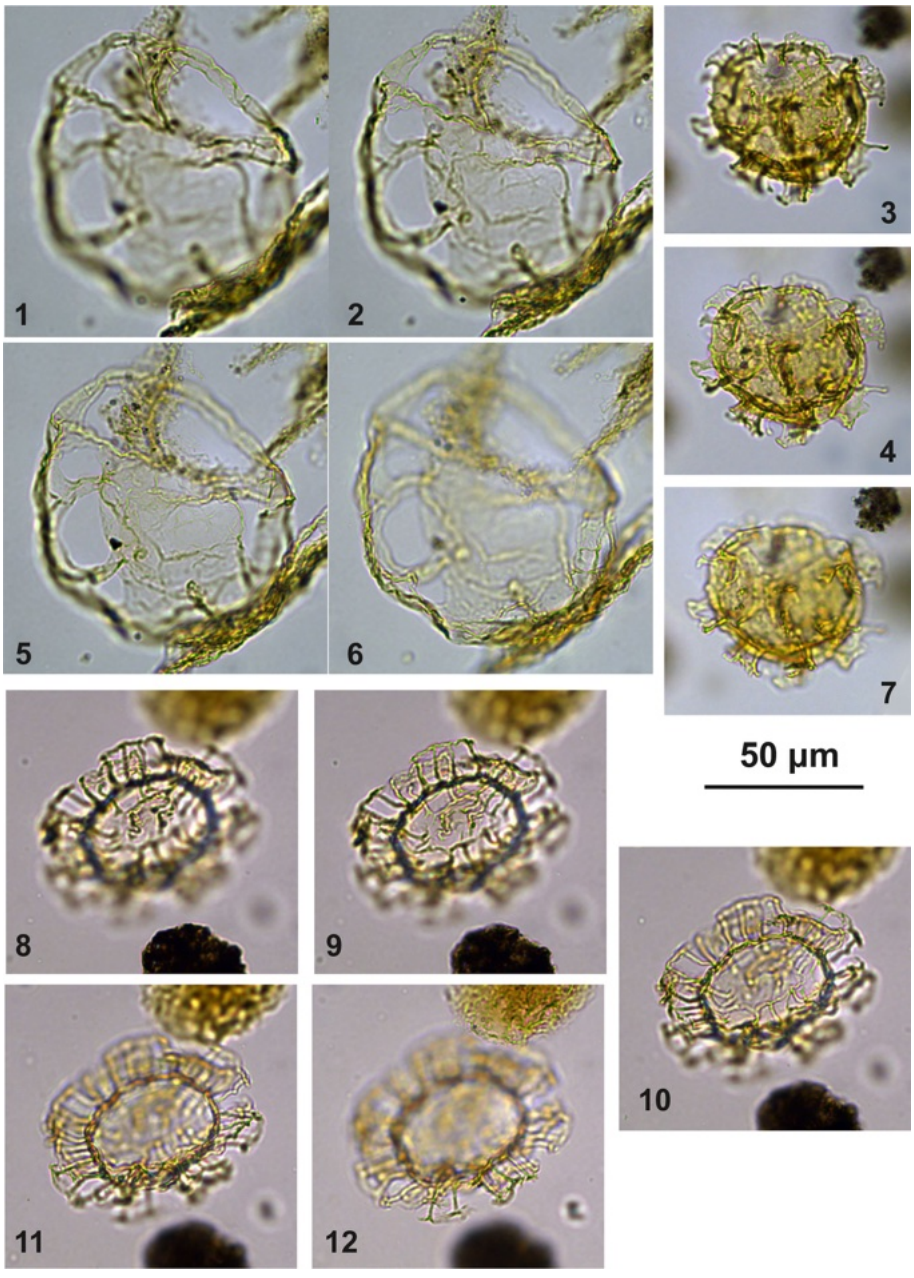

Plate C6. **(1–2, 5–6)** *Guersteinia*? *sluijsii* sp. nov.; sample A900, slide 2, EF: F20/1. **(3, 4, 7)** *Cooksonidium* group; sample A000, slide 2, EF: J31. **(8–12)** *Bujakidinium umbellum* gen. nov. sp. nov.; sample A060, slide 2, EF: M22.

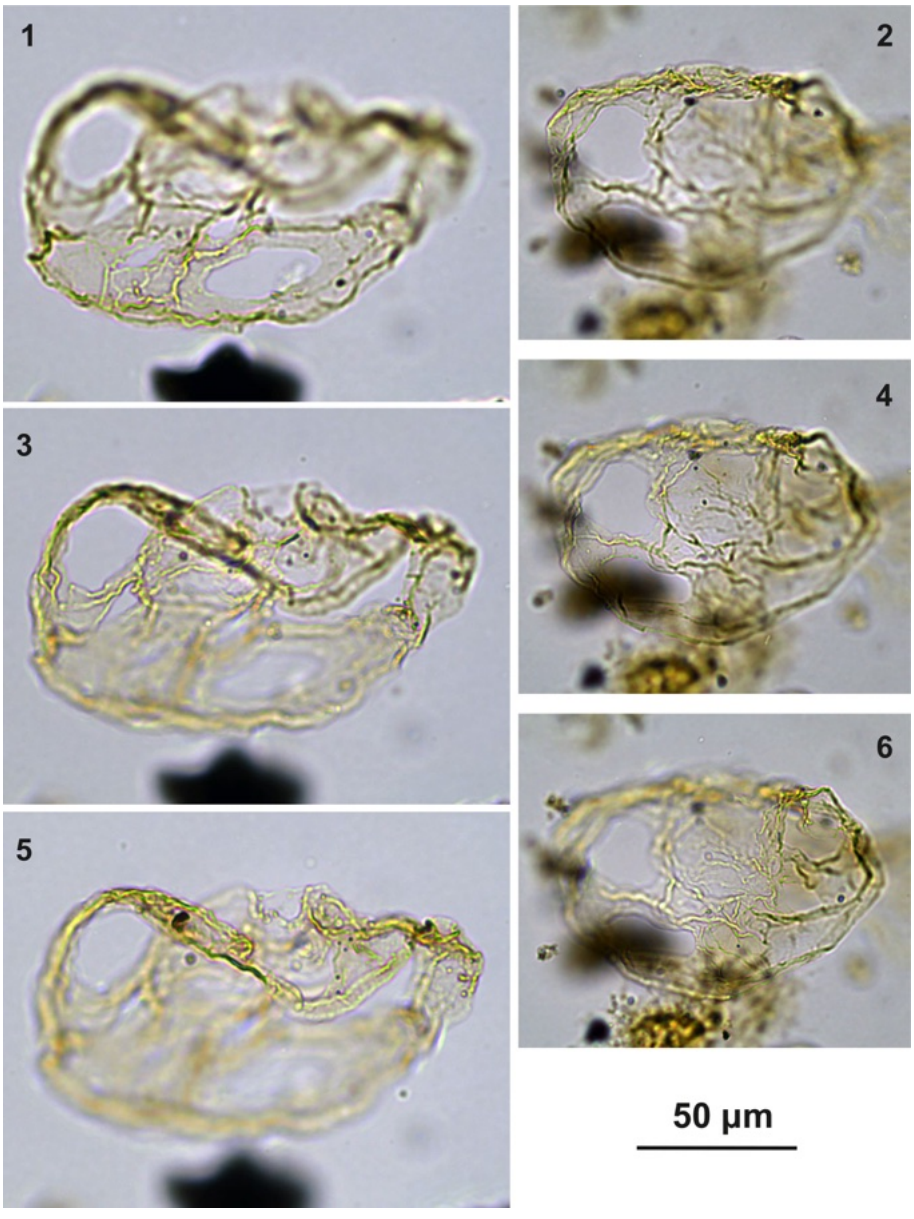

Plate C7. **(1, 3, 5)** *Guersteinia*? *sluijsii* sp. nov.; sample A1200, slide 2, EF: V24/2. **(2, 4, 6)** *Guersteinia*? *sluijsii* sp. nov.; sample A1260, slide 1, EF: J20/1.

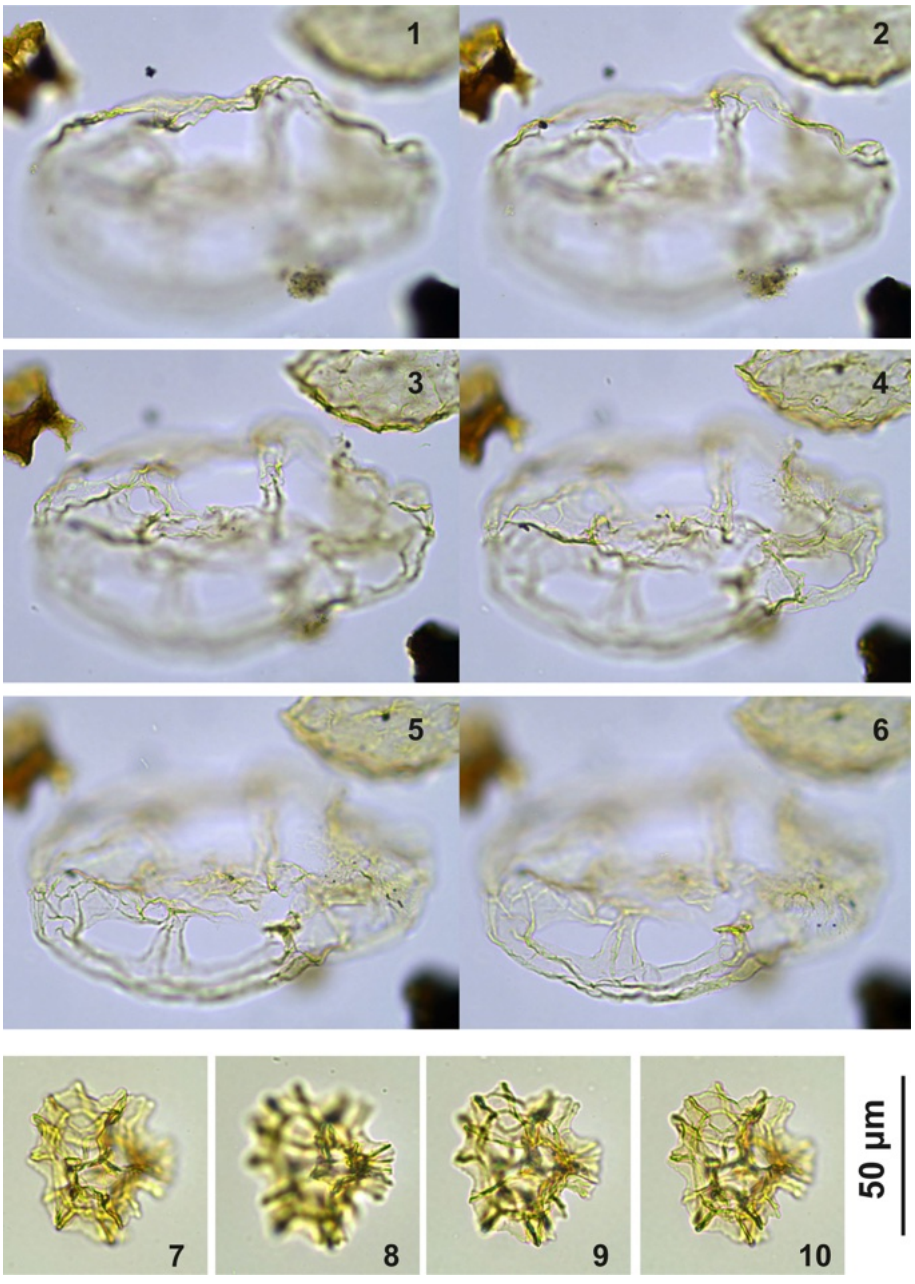

Plate C8. **(1–6)** *Guersteinia*? *sluijsii* sp. nov.; sample A5512, slide 1, EF: S17/4. **(7–10)** *Impagidinium gedlii* sp. nov.; sample A3718, slide 1, EF: O30/4.

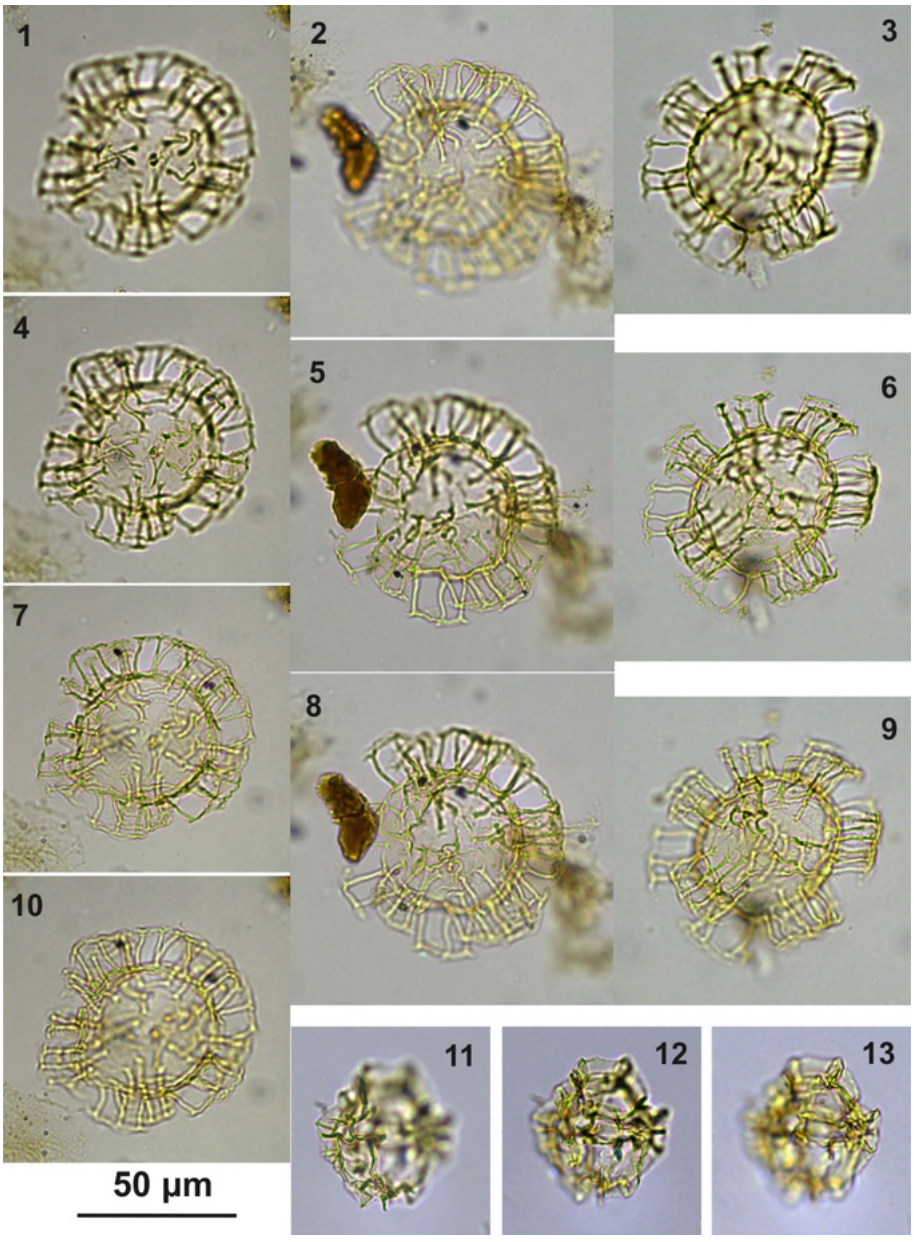

Plate C9. **(1, 4, 7, 10)** *Bujakidinium umbellum* gen. nov. sp. nov., paratype; sample A060, slide 2, EF: N22. **(2, 5, 8)** *Bujakidinium umbellum* gen. nov. sp. nov., holotype; sample A000, slide 2, EF: V30. **(3, 6, 9)** *Bujakidinium umbellum* gen. nov. sp. nov.; sample A120, slide 2, EF: P28/4. **(11–13)** *Impagidinium gedlii* sp. nov.; sample A000, slide 2, EF: W18/3.

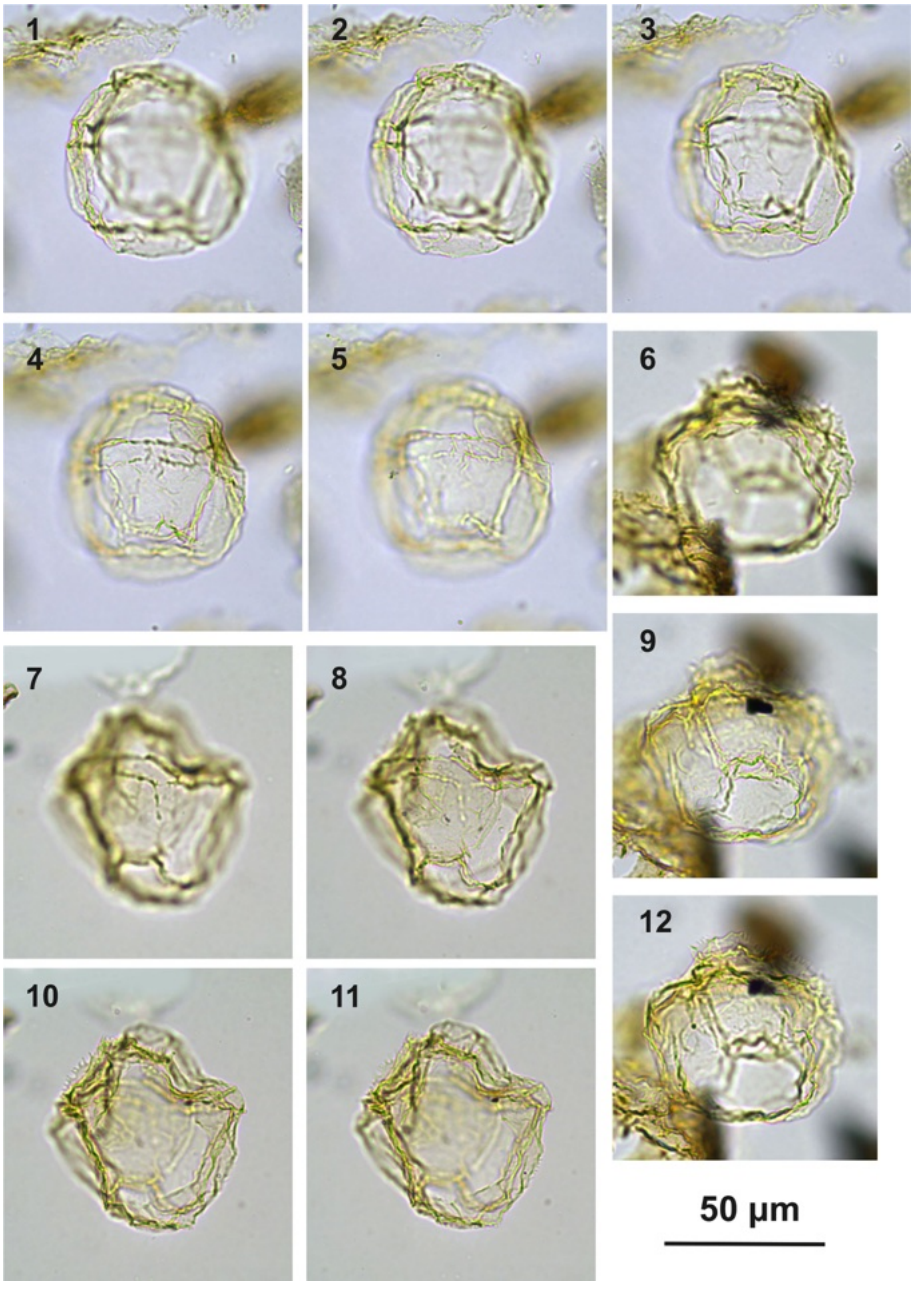

Plate C10. **(1–5)** *Guersteinia châteauneufii* sp. nov., paratype; sample A3918, slide 1, EF: F34. **(6, 9, 12)** *Guersteinia châteauneufii* sp. nov., sample A720, slide 1, EF: D29/3. **(7–8, 10–11)** *Guersteinia châteauneufii* sp. nov., holotype; sample A780, slide 1, EF: P22/2.

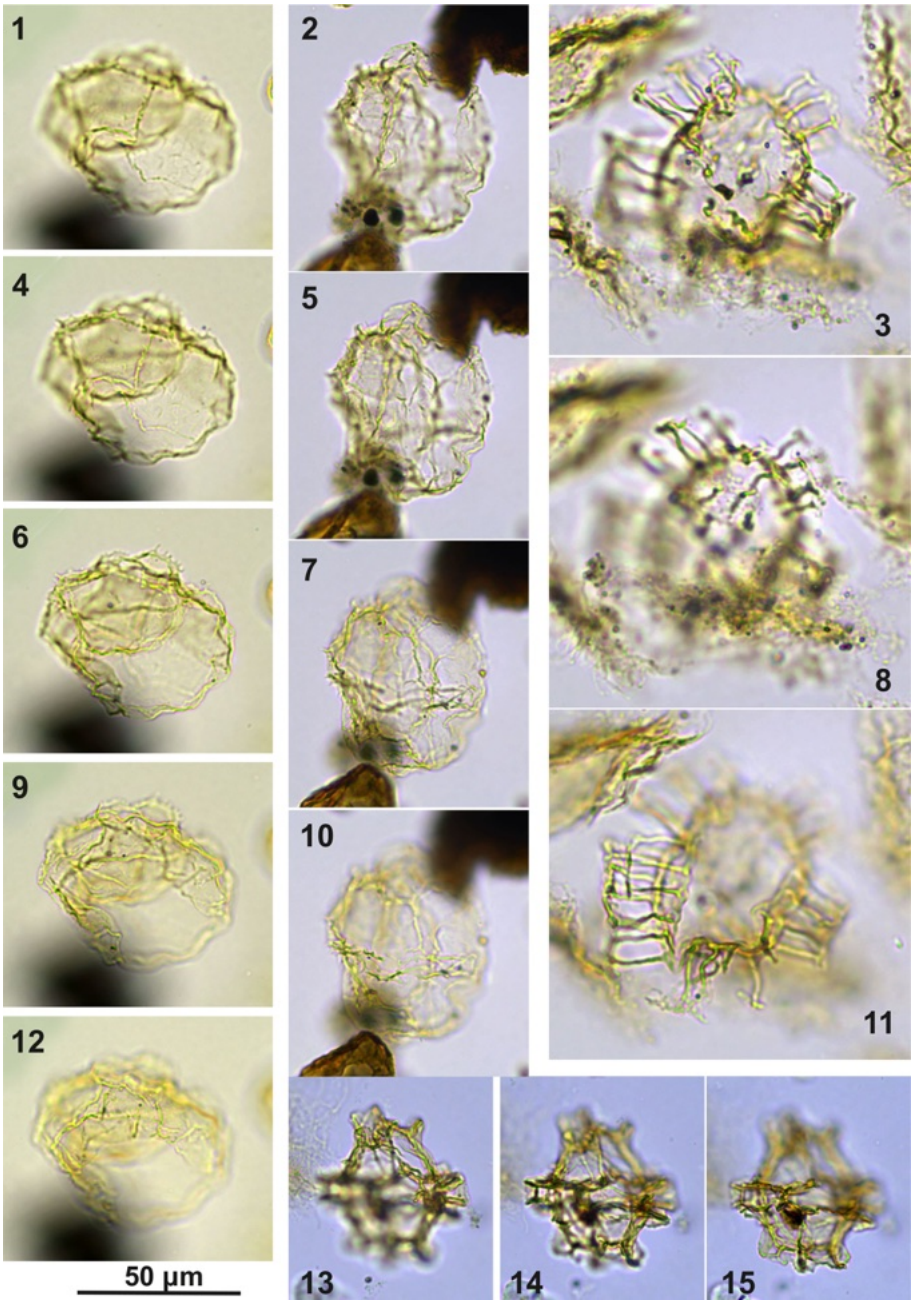

Plate C11. **(1, 4, 6, 9, 12)** *Guersteinia châteauneufii* sp. nov., sample A5752, slide 2, EF: H28. **(2, 5, 7, 10)** *Guersteinia châteauneufii* sp. nov., sample A5812, slide 1, EF: E31/1. **(3, 8, 11)** *Bujakidinium umbellum* gen. nov. sp. nov.; sample A4658, slide 2, EF: Q14/2. **(13–15)** *Impagidinium gedlii* sp. nov.; sample A3030, slide 2, EF: Q33.

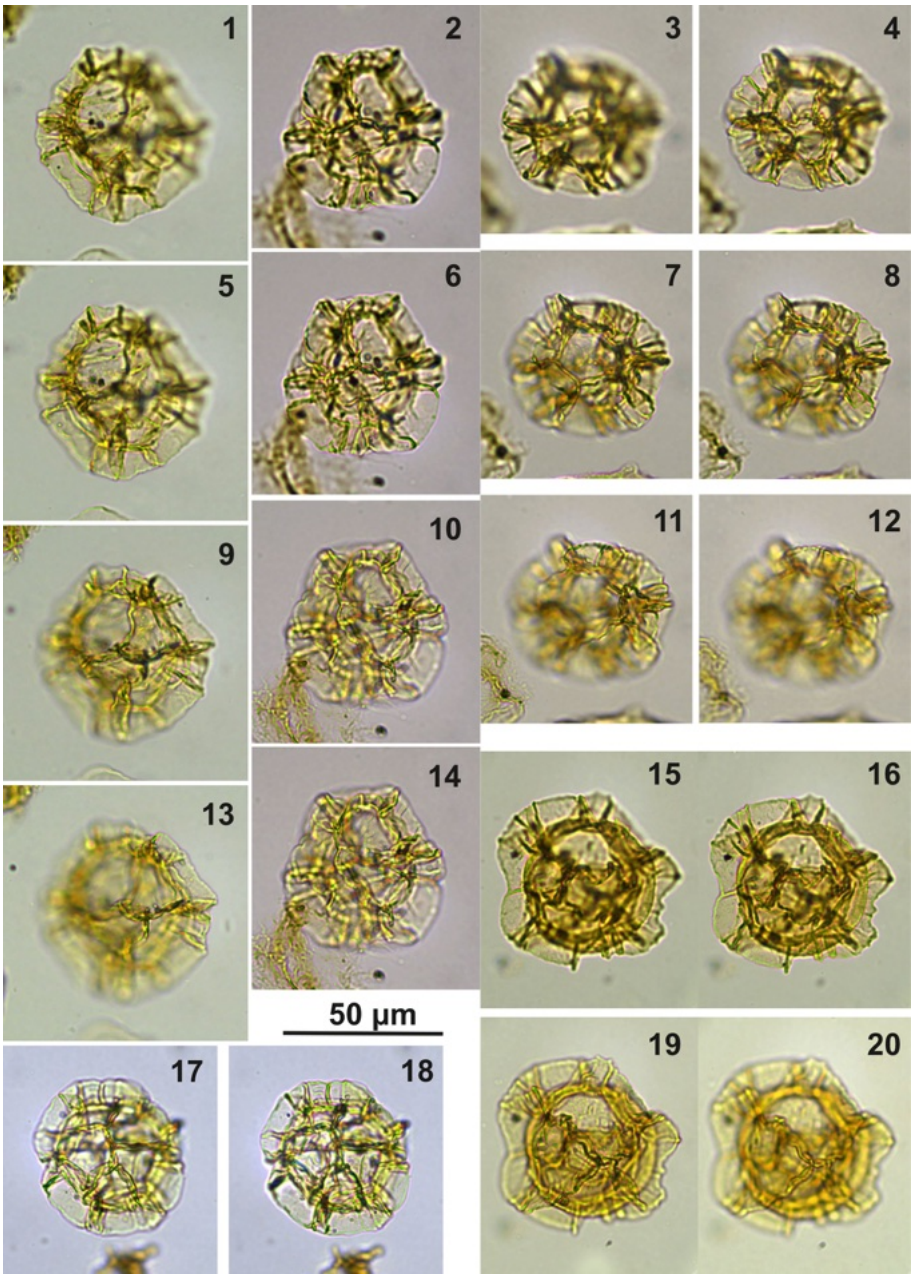

Plate C12. **(1, 5, 9, 13)** *Impagidinium gedlii* sp. nov., holotype; sample A240, slide 1, EF: V28. **(2, 6, 10, 14)** *Impagidinium gedlii* sp. nov., paratype; sample A1260, slide 1, EF: T18/2. **(3–4, 7–8, 11–12)** *Impagidinium gedlii* sp. nov.; sample A1200, slide 2, EF: P30/4. **(15–16, 19–20)** *Impagidinium gedlii* sp. nov.; sample A240, slide 1, EF: M25/3. **(17–18)** *Impagidinium gedlii* sp. nov.; sample A10069, slide 2, EF: Q20.

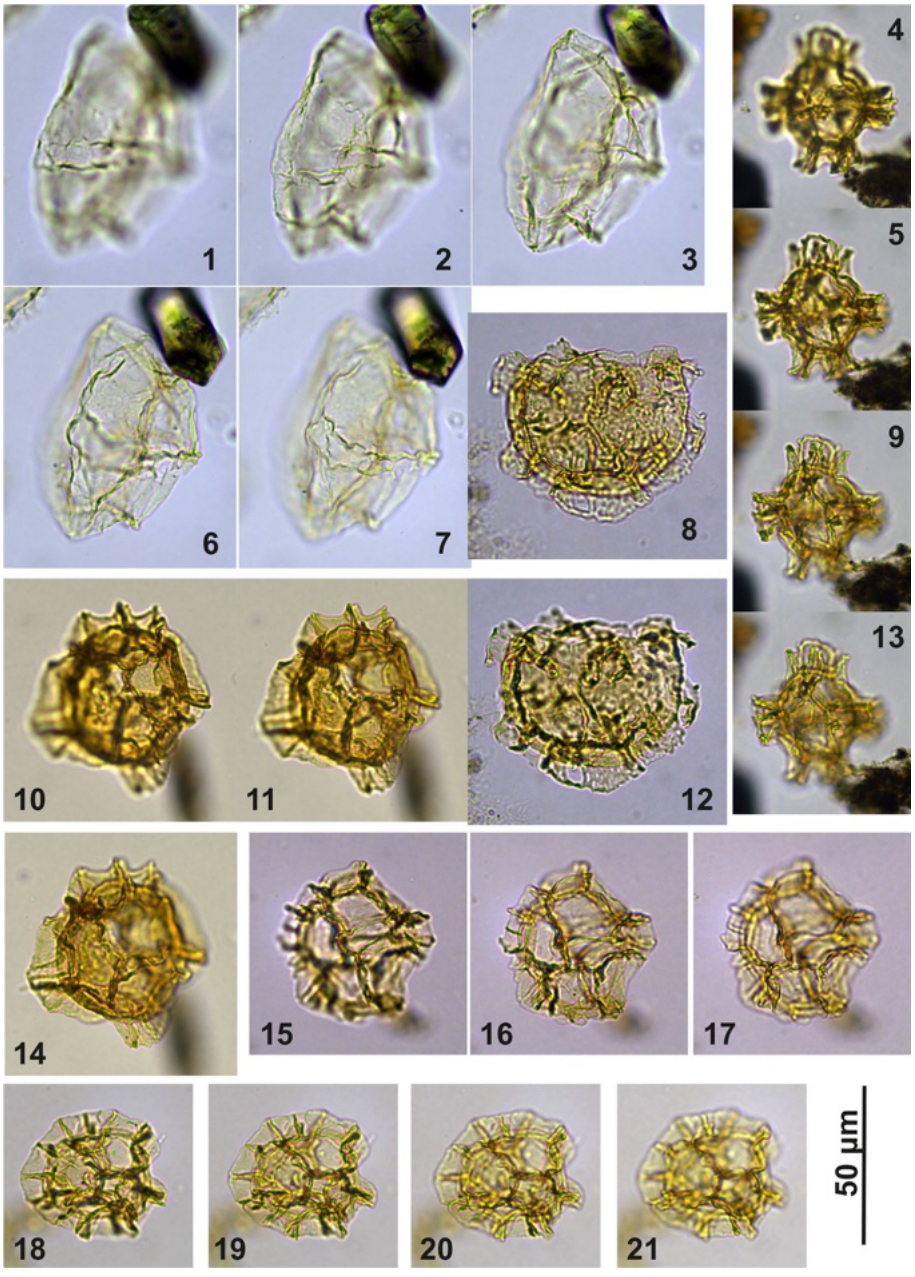

Plate C13. **(1–3, 6–7)** *Guersteinia châteauneufii* sp. nov.; sample A6295, slide 2, EF: F15/4. **(4–5, 9, 13)** *Impagidinium gedlii* sp. nov.; sample A840, slide 1, EF: F27/3. **(8, 12)** *Cooksonidium* group; sample A000, slide 2, EF: U18/4. **(10–11, 14)** *Impagidinium gedlii* sp. nov.; sample A120, slide 2, EF: R20/4. **(15–17)** *Impagidinium gedlii* sp. nov.; sample A060, slide 2, EF: G22/1. **(18–21)** *Impagidinium gedlii* sp. nov.; sample A1200, slide 2, EF: R14/2.

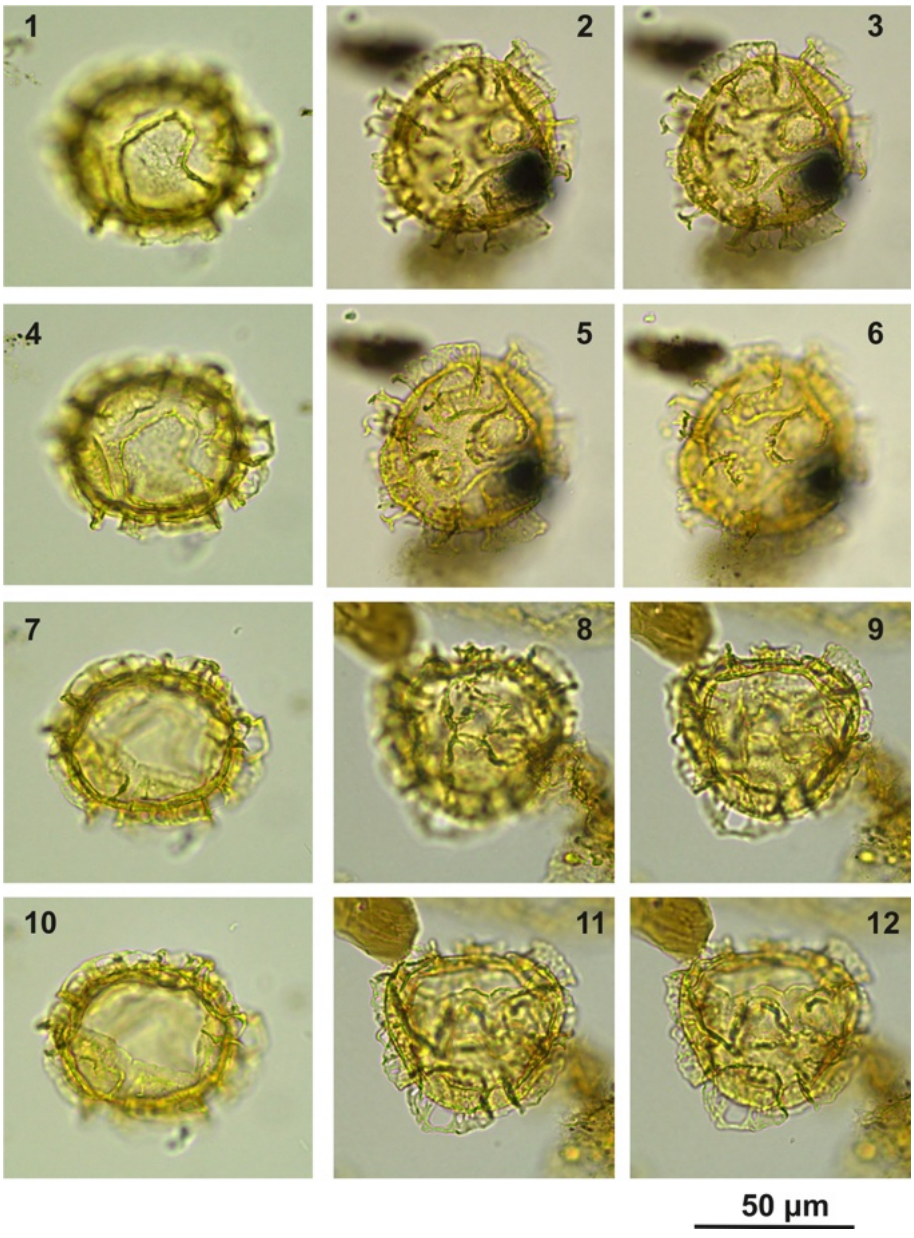

Plate C14. **(1, 4, 7, 10)** *Cooksonidium* group; sample A4283, slide 2, EF: V22. **(2–3, 5–6)** *Cooksonidium* group; sample A000, slide 2, EF: Q25. **(8–9, 11–12)** *Cooksonidium* group; sample A4283, slide 2, EF: T24.

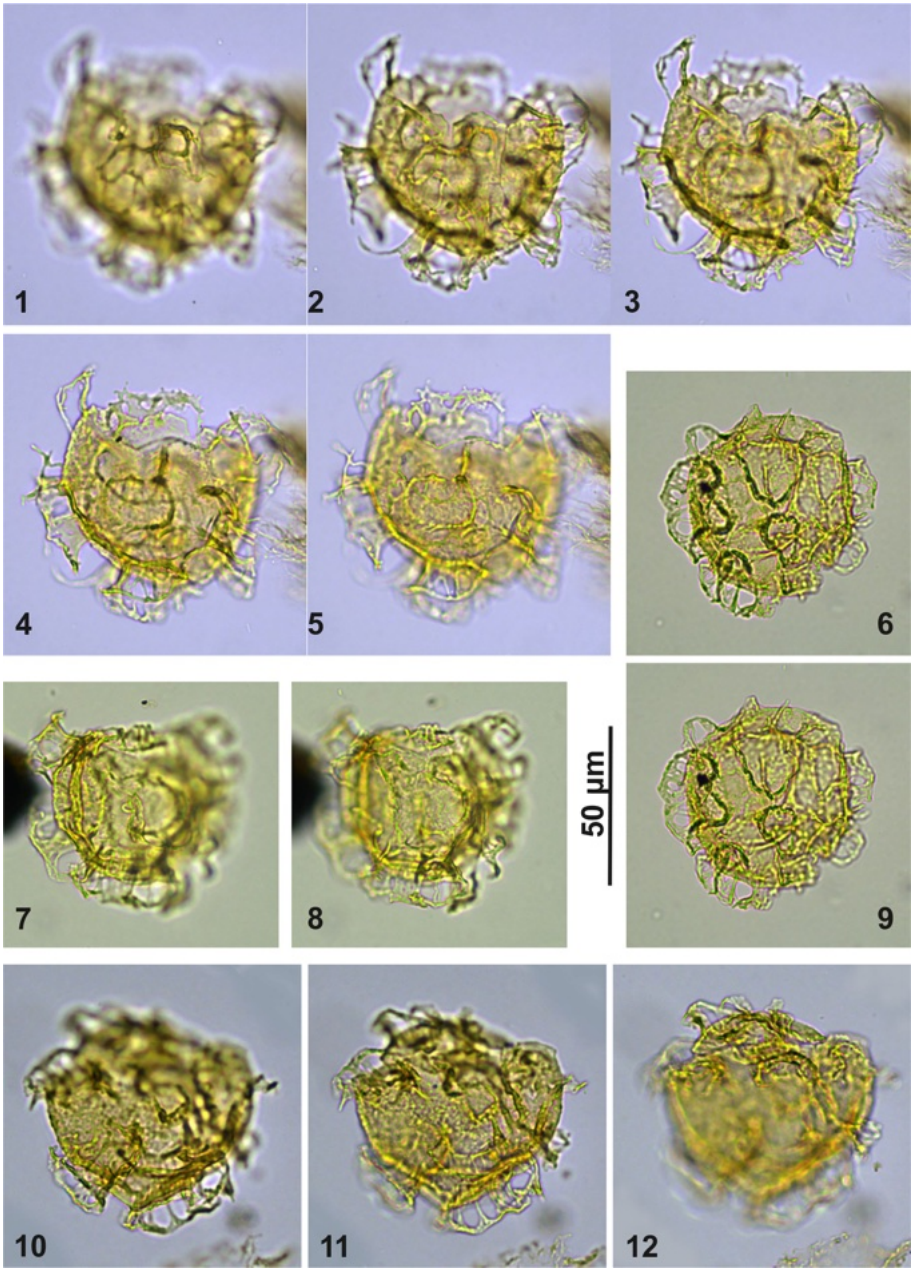

Plate C15. **(1–5)** *Cooksonidium* group; sample A10309, slide 2, EF: Q33/1. **(6, 9)** *Cooksonidium* group; sample A4283, slide 2, EF: O23. **(7–8)** *Cooksonidium* group; sample A4158, slide 1, EF: D21/3. **(10–12)** *Cooksonidium* group; sample A000, slide 2, EF: L33/1.

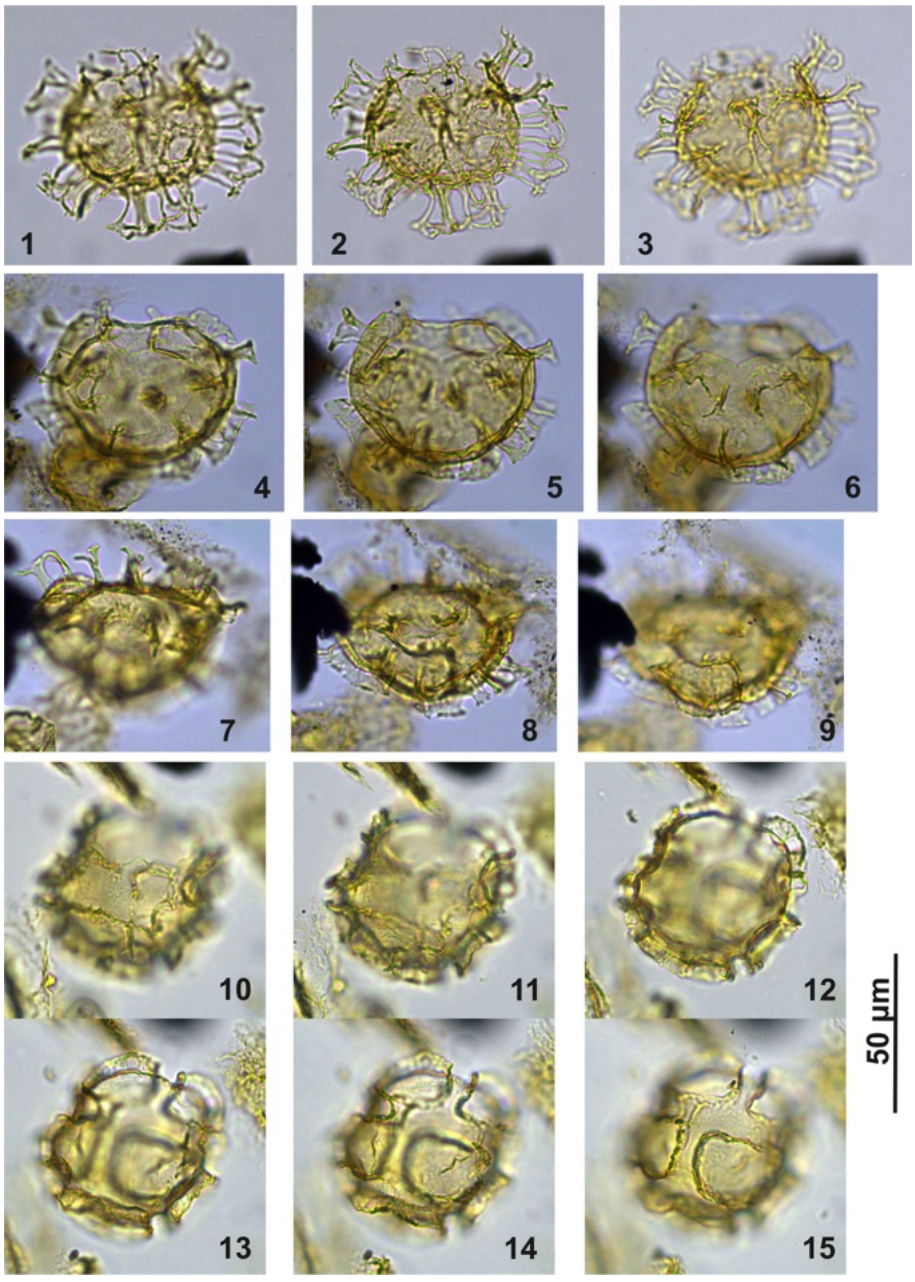

Plate C16. **(1–3)** *Cooksonidium* group; sample A1380, slide 2, EF: M167/2. **(4–6)** *Cooksonidium* group; sample A000, slide 2, EF: O15. **(7–9)** *Cooksonidium* group; sample A000, slide 2, EF: L16/2. **(10–15)** *Cooksonidium* group; sample A4407, slide 2, EF: U22/1.

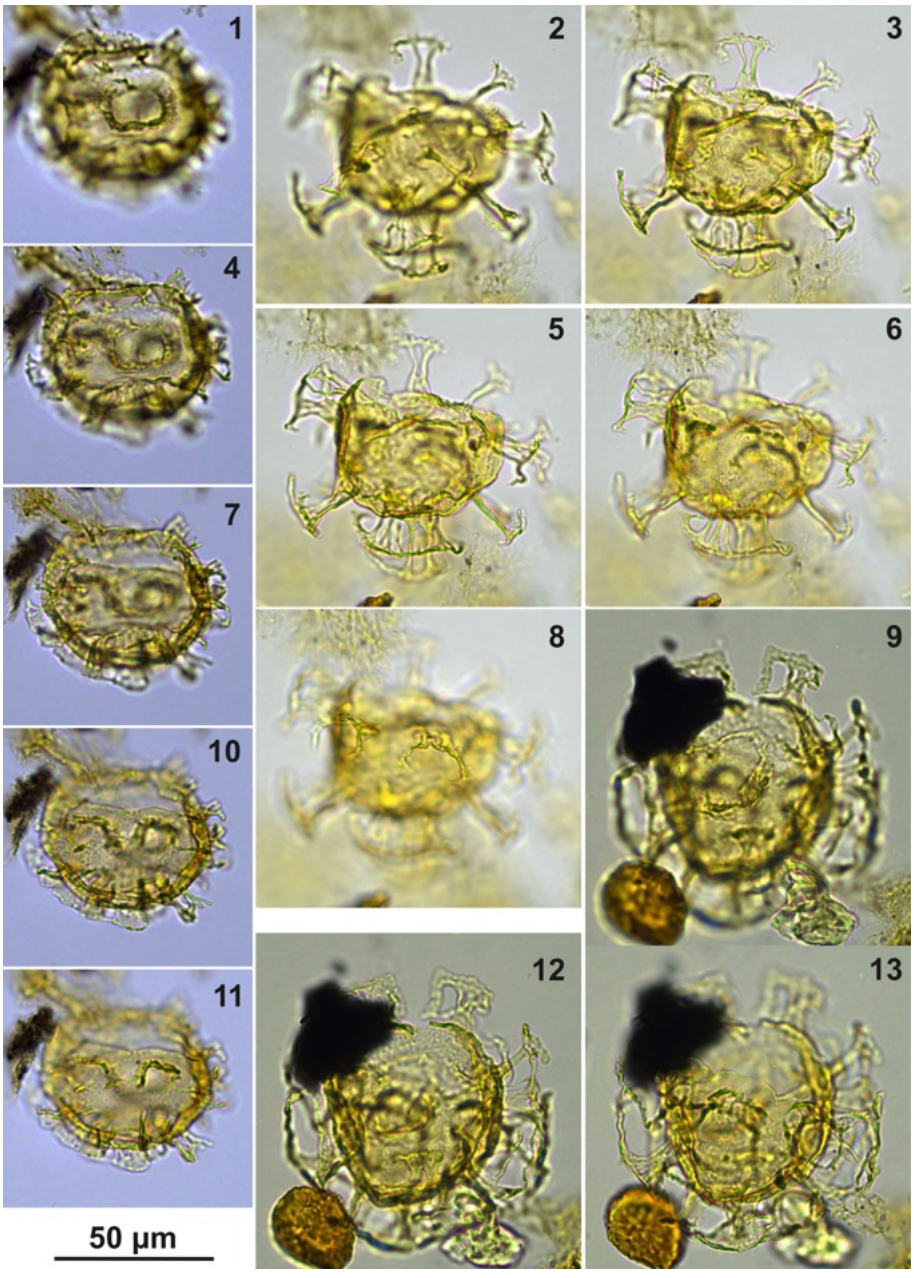

Plate C17. **(1, 4, 7, 10–11)** *Cooksonidium* group; sample A000, slide 2, EF: J17/2. **(2–3, 5–6, 8)** *Cooksonidium* group; sample A7081, slide 2, EF: M20/1. **(9, 12–13)** *Cooksonidium* group; sample A4158, slide 1, EF: J23/3.

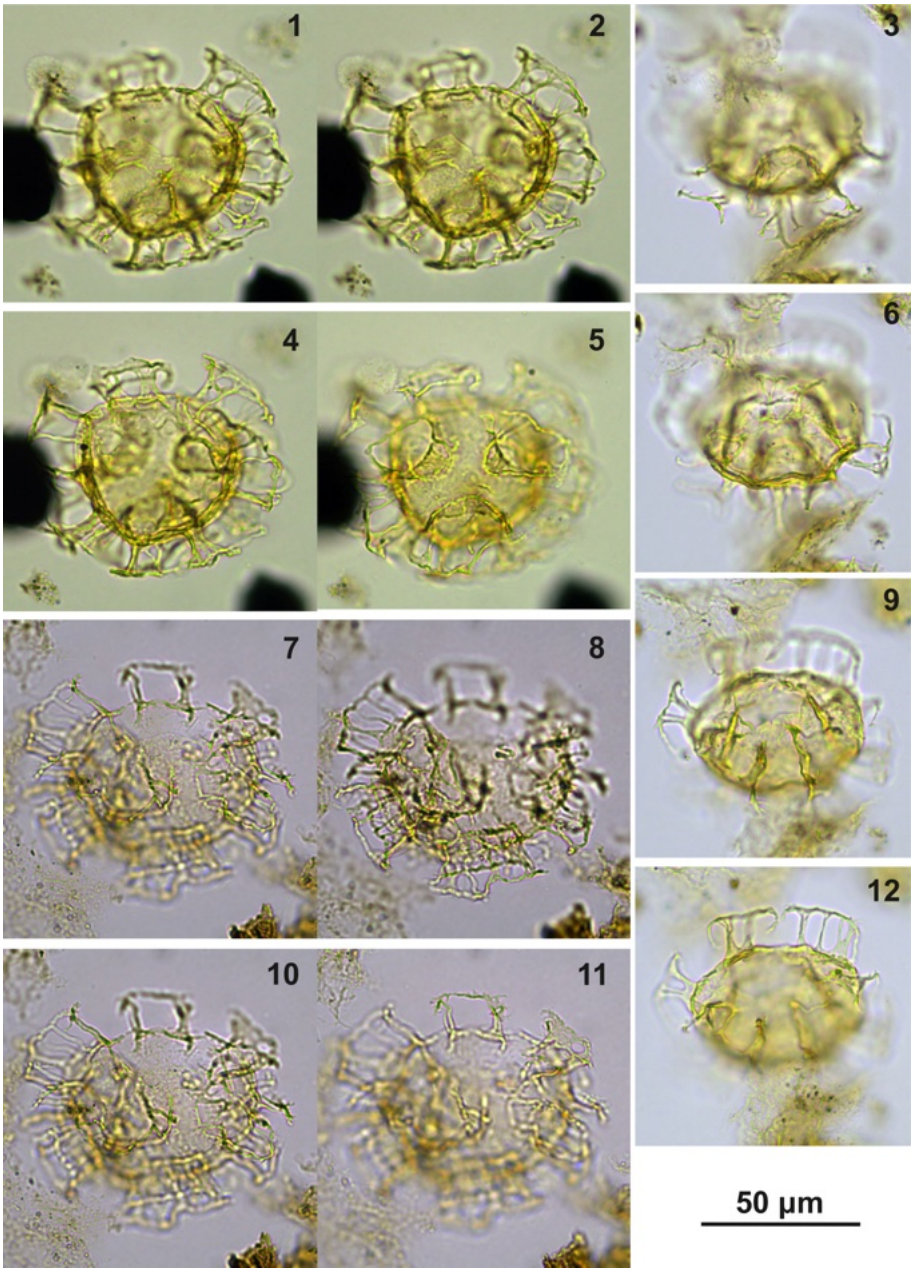

Plate C18. **(1–2, 4–5)** *Cooksonidium* group; sample A4158, slide 1, EF: J32/4. **(3, 6, 9, 12)** *Cooksonidium* group; sample A8401, slide 2, EF: J14/4. **(7–8, 10–11)** *Cooksonidium* group; sample A960, slide 1, EF: F28/4.

Data availability. The microscope slides are stored at Utrecht University. The datasets for this article can be found at https://doi.org/10.5281/zenodo.19338992 (Houben et al., 2026).

Supplement. The supplement related to this article is available online at https://doi.org/10.5194/jm-45-219-2026-supplement.

Author contributions. The research was designed by AH, HB, and AI. The palynological analysis was carried out by AH, AI, and HB. AI and HB provided the photomicrographs and taxonomic descriptions. SG carried out the cyclostratigraphic analysis. AH compiled the article, with input from all of the authors.

Competing interests. The contact author has declared that none of the authors has any competing interests.

Acknowledgements. We thank Natasja Welters and Jan van Tongeren (UU, MPP) for the sample processing. The research of AI was supported by the State program of the Geological Institute of the Russian Academy of Sciences.

Review statement. This paper was edited by Luke Mander and reviewed by Stefano Torricelli and Manuel Vieira.

References

Abbink, O. A., Van Konijnenburg-Van Cittert, J. H. A., and Visscher, H.: A sporomorph ecogroup model for the Northwest European Jurassic-Lower Cretaceous: concepts and framework, Netherlands Journal of Geosciences, 83, 17–31, 2004.

Agelopoulos, J.: *Hystrichostrogylon membraniphorum* n.g. n.sp. aus dem Heiligenhafener Kieselton (Eozän), Neues Jahrbuch für Geologie und Paläontologie, Monatshefte, 11, 673–675, 1964.

Agnini, C., Fornaciari, E., Raffi, I., Catanzariti, R., Pälike, H., Backman, J., and Rio, D.: Integrated biomagnetostratigraphy of the Alano section (NE Italy): a proposal for defining the Middle-Late Eocene boundary. Geological Society of America Bulletin, 123, 841–872, https://doi.org/10.1130/B30432.1, 2011.

Agnini, C., Backman, J., Fornaciari, E., Galeotti, S., Giusberti, L., Grandesso, P., Lanci, L., Rio, D., and Stefani, C.: The Alano section: the candidate GSSP for the Priabonian stage, in: First International Congress on Stratigraphy At the Cutting Edge of Stratigraphy, edited by: Rocha, R., Pais, J., Kullberg, J. C., and Finney, S., Strati 2013, Springer International Publishing, Cham, 55–59, 2014.

Agnini, C., Muttoni, G., Giusberti, L., Fornaciari, E., Rio, D., Spofforth, D. J. A., Pälike, H., Backman, J., Condon, D. J., Lanci, L., and Stefani, C.: Proposal for the global boundary stratotype section and point (GSSP) for the Priabonian stage (Eocene) at the Alano section (Italy), Episodes Journal of International Geoscience, 44, 151–173, https://doi.org/10.18814/epiiugs/2020/020074, 2021.

Alberti, G.: Zur Kenntnis Mesozoischer und Alttertiärer Dinoflagellaten und Hystrichosphaerideen von Nord- und Mitteldeutschland sowie einigen anderen Europäischen Gebieten, Palaeontographica, Abteilung A, 116, 1–58, 1961.

Bati, Z.: Dinoflagellate cyst biostratigraphy of the upper Eocene and lower Oligocene of the Kirmizitepe Section, Azerbaijan, South Caspian Basin, Review of Palaeobotany and Palynology, 217, 9–38, https://doi.org/10.1016/j.revpalbo.2015.02.001, 2015.

Benedek, P. N.: Phytoplanktonten aus dem Mittel- und Oberoligozän von Tönisberg (Niederrheingebiet), Palaeontographica, Abteilung B, 137, 1–71, 1972.

Bijl, P. K.: DINOSTRAT: a global database of the stratigraphic and paleolatitudinal distribution of Mesozoic–Cenozoic organic-walled dinoflagellate cysts, Earth System Science Data, 14, 579–617, https://doi.org/10.5194/essd-14-579-2022, 2022.

Bijl, P. K., Brinkhuis, H., Egger, L. M., Eldrett, J. S., Frieling, J., Grothe, A., Houben, A. J. P., Pross, J., Śliwińska, K. K., and Sluijs, A.: Comment on "*Wetzeliella*" and its allies – the "hole" story: a taxonomic revision of the Paleogene dinoflagellate subfamily Wetzelielloideae' by Williams et al. (2015), Palynology, 42, 66–72, https://doi.org/10.1080/01916122.2017.1283367, 2017.

Bohaty, S. M. and Zachos, J. C.: Significant Southern Ocean warming event in the late middle Eocene, Geology, 31, 1017–1020, https://doi.org/10.1130/G19800.1, 2003.

Bohaty, S. M., Zachos, J. C., Florindo, F.. and Delaney, M. L.: Coupled greenhouse warming and deep-sea acidification in the middle Eocene, Paleoceanography, 24, https://doi.org/10.1029/2008PA001676, 2009.

Bosellini, A.: Dynamics of Tethyan carbonate platforms, in: Controls on Carbonate Platform and Basin Development, edited by: Crevello, P. D., Wilson, J. L., Sarg, J. F., and Read, J. F., SEPM Special Publication 44, Society for Sedimentary Geology, Tulsa, 1989.

Brinkhuis, H.: Late Paleogene dinoflagellate cysts with special reference to the Eocene/Oligocene boundary, in: Eocene–Oligocene Climatic and Biotic Evolution, edited by: Prothero, D. R. and Berggren, W. A., Princeton University Press, Princeton, 327–340, 1992.

Brinkhuis, H.: Late Eocene to Early Oligocene dinoflagellate cysts from the Priabonian type-area (Northeast Italy): biostratigraphy and paleoenvironmental interpretation, Palaeogeography, Palaeoclimatology, Palaeoecology, 107, 121–163, 1994.

Brinkhuis, H. and Biffi, U.: Dinoflagellate cyst stratigraphy of the Eocene/Oligocene transition in central Italy, Marine Micropaleontology, 22, 131–183, 1993.

Brinkhuis, H., Fioroni, C., and Kaya, M. Y.: There and back again; on dinoflagellate cyst "index events'; of the Eocene Oligocene Transition in the (Para) Tethyan Realm, Review of Palaeobotany and Palynology, 343, 105414, https://doi.org/10.1016/j.revpalbo.2025.105414, 2025.

Brosius, M.: Plankton aus dem nordhessischen Kasseler Meeressand (Oberoligozän), Zeitschrift der Deutschen Geologischen Gesellschaft, 114, 32–56, 1963.

Bujak, J. P.: An evolutionary series of Late Eocene dinoflagellate cysts from southern England, Mar. Micropaleontol., 1, 101–117, https://doi.org/10.1016/0377-8398(76)90007-4, 1976.

Bujak, J. P.: Dinoflagellate cysts and acritarchs from the Eocene Barton Beds of southern England, in: Dinoflagellate cysts and acritarchs from the Eocene of southern England, edited by: Bujak, J. P., Downie, C., Eaton, G. L., and Williams, G. L., Special Papers in Palaeontology, 24, 36–91, 1980.

Bujak, J. P.: Cenozoic dinoflagellate cysts and acritarchs from the Bering Sea and northern North Pacific, D.S.D.P. Leg 19, Micropaleontology, 30, 180–212, 1984.

Bujak, J. P.: New dinocyst taxa from the Eocene of the North Sea, Journal of Micropalaeontology, 13, 119–131, 1994.

Bujak, J. P. and Matsuoka, K.: Taxonomic reallocation of Cenozoic dinoflagellate cysts from Japan and the Bering Sea, Palynology, 10, 235–241, 1986.

Bütschli, O.: Erster Band. Protozoa, in: Dr. H.G. Bronn's Klassen und Ordnungen des Thier-Reichs, wissenschaftlich dargestellt in Wort und Bild, C.F. Winter'sche Verlagsbuchhandlung, Leipzig and Heidelberg, 865–1088, 1885.

Châteauneuf, J.-J. and Gruas-Cavagnetto, C.: Les zones de Wetzeliellaceae (Dinophyceae) du bassin de Paris. Comparaison et corrélations avec les zones du Paléogène des bassins du nord-ouest de l'Europe, Bulletin du Bureau des recherches géologiques et minières, 2, 59–93, 1978.

Cookson, I. C.: Cretaceous and Tertiary microplankton from southeastern Australia, Proceedings of the Royal Society of Victoria, 78, 85–93, 1965.

Cookson, I. C. and Eisenack, A.: Tertiary microplankton from the Rottnest Island Bore, Western Australia, Journal of the Royal Society of Western Australia, 44, 39–47, 1961.

Cookson, I. C. and Eisenack, A.: Microplankton from the Browns Creek Clays, sw. Victoria, Proceedings of the Royal Society of Victoria, 79, 119–131, 1965.

Cookson, I. C. and Eisenack, A.: Some microplankton from the Paleocene Rivernook Bed, Victoria, Proceedings of the Royal Society of Victoria, 80, 247–257, 1967.

Costa, L. I. and Downie, C.: The Wetzeliellaceae; Palaeogene dinoflagellates, in: Proceedings of the 4th International Palynological Conference, Lucknow (1976–77), v.2, 34–46, 1979.

Cramwinckel, M. J., Coxall, H. K., Śliwińska, K. K., Polling, M., Harper, D. T., Bijl, P. K., Reichart, G.-J., Schouten, S., and Sluijs, A.: A warm, stratified, and restricted Labrador Sea across the Middle Eocene and its climatic optimum, Paleoceanography and Paleoclimatology, 35, https://doi.org/10.1029/2020PA003932, 2020.

Damassa, S. P.: Eocene dinoflagellates from the Coastal Belt of the Franciscan Complex, northern California, Journal of Paleontology, 53, 815–840, 1979.

Davey, R. J. and Williams, G. L.: IV. The genera *Hystrichosphaera* and *Achomosphaera*, in: Studies on Mesozoic and Cainozoic dinoflagellate cysts, edited by: Davey, R. J., Downie, C., Sarjeant, W. A. S., and Williams, G. L., British Museum (Natural History) Geology, Bulletin, Supplement 3, 28–52, 1966.

Deflandre, G. and Cookson, I. C.: Fossil microplankton from Australian Late Mesozoic and Tertiary sediments, Australian Journal of Marine and Freshwater Research, 6, 242–313, 1955.

Drugg, W. S.: Some new genera, species, and combinations of phytoplankton from the Lower Tertiary of the Gulf Coast, U.S.A., Proceedings of the North American Paleontological Convention, Chicago, September 1969, Part G, 809–843, 1970.

Drugg, W. S. and Loeblich, A. R. Jr.: Some Eocene and Oligocene phytoplankton from the Gulf Coast, U.S.A., Tulane Studies in Geology, 5, 181–194, 1967.

Eaton, G. L.: A morphogenetic series of dinoflagellate cysts from the Bracklesham Beds of the Isle of Wight, Hampshire, England, in: Proceedings of the 2nd Planktonic Conference, Rome, 1970, edited by: Farinacci, A., Edizioni Tecnoscienza, Rome, 355–379, 1971.

Eaton, G. L.: Dinoflagellate cysts from the Bracklesham Beds (Eocene) of the Isle of Wight, southern England, British Museum (Natural History) Geology, Bulletin, 26, 227–332, 1976.

Edwards, L. E.: Biostratigraphically important species of *Pentadinium* Gerlach 1961 and a likely ancestor, *Hafniasphaera goodmanii* n. sp. and from the Eocene of the Atlantic and Gulf coastal plains, Palynology, 6, 105–117, https://doi.org/10.1080/01916122.1982.9989237, 1982.

Edwards, L. E.: Dinocyst biostratigraphy of Tertiary sediments from five cores from Screven and Burke counties, Georgia, in: Geology and paleontology of five cores from Screven and Burke counties, eastern Georgia, edited by: Edwards, L. E., United States Geological Survey Professional Paper, 1603, G1–G25, https://doi.org/10.3133/pp1603G, 2001.

Ehrenberg, C. G.: Über das Massenverhältniss der jetzt lebenden Kiesel-Infusorien und über ein neues Infusorien-Conglomerat als Polirschiefer von Jastraba in Ungarn, Abhandlungen der Königlichen Akademie der Wissenschaften zu Berlin, Physikalische Klasse, 109–135, 1837.

Eisenack, A.: Die Phosphoritknollen der Bernsteinformation als Überlieferer tertiären Planktons, Schriften der Physikalisch-Ökonomischen Gesellschaft zu Königsberg, 70, 181–188, 1938.

Eisenack, A.: Mikrofossilien aus Phosphoriten des samländischen Unteroligozäns und über die Einheitlichkeit der Hystrichosphaerideen, Palaeontographica, Abteilung A, 105, 49–95, 1954.

Eisenack, A.: Kritische Bemerkungen und Richtigstellungen im Gebiet der fossilen Dinoflagellaten und Acritarchen, Neues Jahrbuch für Geologie und Paläontologie, Abhandlungen, 134, 101–116, 1969.

Eisenack, A. and Gocht, H.: Neue Namen für einige Hystrichosphären der Bernsteinformation Ostpreussens, Neues Jahrbuch für Geologie und Paläontologie, Monatshefte, 11, 511–518, 1960.

Eisenack, A. and Kjellström, G.: Katalog der Fossilen Dinoflagellaten, Hystrichosphären und Verwandten Mikrofossilien. Band I. Dinoflagellaten. 2. Ergänzungslieferung, E. Schweizerbart'sche Verlagsbuchhandlung, Stuttgart, 215 pp., 1971.

Fensome, R. A., Taylor, F. J. R., Norris, G., Sarjeant, W. A. S., Wharton, D. I., and Williams, G. L.: A classification of fossil and living dinoflagellates, Micropaleontology Press Special Paper, 7, 351 pp., 1993.

Fensome, R. A., Williams, G. L., and MacRae, R. A.: Late Cretaceous and Cenozoic fossil dinoflagellates and other palynomorphs from the Scotian Margin, offshore eastern Canada, Journal of Systematic Palaeontology, 7, 1–79, https://doi.org/10.1017/S147720190800262X, 2009.

Fensome, R. A., Williams, G. L., and MacRae, R. A.: The Lentin and Williams index of fossil dinoflagellates edition 2019, American Association of Stratigraphic Palynologists Contribution Series 50, 1173, https://palynologyshop.org/product/the-lentin-and-williams-index-of-fossil-dinoflagellates-2019 (last access: 10 March 2026), 2019.

Fokkema, C. D., Buijs, S., Bialik, O. M., Meilijson, A., Waldmann, N. D., Makovsky, Y., and Sluijs, A.: Late Paleocene to middle Eocene carbon isotope stratigraphy of the Northern Negev, Southern Israel: potential for paleoclimate reconstructions, Newsletters on Stratigraphy, 55, 361–384, https://doi.org/10.1127/nos/2022/0684, 2022.

Frieling, J. and Sluijs, A.: Towards quantitative environmental reconstructions from ancient non-analogue microfossil assemblages: Ecological preferences of Paleocene–Eocene dinoflagellates, Earth-Science Reviews, 185, 956–973, https://doi.org/10.1016/j.earscirev.2018.08.014, 2018.

Galazzo, F. B., Giusberti, L., Luciani, V., and Thomas, E.: Paleoenvironmental changes during the Middle Eocene Climatic Optimum (MECO) and its aftermath: The benthic

foraminiferal record from the Alano section (NE Italy), Palaeogeography, Palaeoclimatology, Palaeoecology, 378, 22–35, https://doi.org/10.1016/j.palaeo.2013.03.018, 2013.

Galeotti, S., Sahy, D., Agnini, C., Condon, D., Fornaciari, E., Francescone, F., Giusberti, L., Guasti, E., Jutson, D., Lanci, L., Pälike, H., Spofforth, D. J. A., and Rio, D.: Astrochronology and radio-isotopic dating of the Alano di Piave section (NE Italy), candidate GSSP for the Priabonian Stage (late Eocene), Earth and Planetary Science Letters, 525, 115746, https://doi.org/10.1016/j.epsl.2019.115746, 2019.

Gedl, P.: Dinoflagellate cyst record of the deep-sea Cretaceous–Tertiary boundary at Uzgruň, Carpathian Mountains, Czech Republic, Studia Geologica Polonica, 123, 243–267, 2004a.

Gedl, P.: Dinoflagellate cyst record of the Eocene–Oligocene boundary succession in flysch deposits at Leluchów, Carpathian Mountains, Poland, Geologica Carpathica, 55, 203–219, 2004b.

Gedl, P.: Late Eocene-early Oligocene organic-walled dinoflagellate cysts from Folusz, Magura Nappe, Polish Carpathians, Acta Palaeobotanica, 45, 27–81, 2005.

Gerlach, E.: Mikrofossilien aus dem Oligozän und Miozän Nordwestdeutschlands, unter besonderer Berücksichtigung der Hystrichosphaeren und Dinoflagellaten, Neues Jahrbuch für Geologie und Paläontologie, Abhandlungen, 112, 143–228, 1961.

Gocht, H.: *Rhombodinium* und *Dracodinium*, zwei neue Dinoflagellaten-Gattungen aus dem norddeutschen Tertiär, Neues Jahrbuch für Geologie und Paläontologie, Monatshefte, 2, 84–92, 1955.

Haiblen, A. M., Opdyke, B. N., Roberts, A. P., Heslop, D., and Wilson, P. A.: Midlatitude southern hemisphere temperature change at the end of the Eocene greenhouse shortly before dawn of the Oligocene icehouse, Paleoceanography and Paleoclimatology, 34, 1995–2004, https://doi.org/10.1029/2019PA003679, 2019.

Head, M. J.: Last Interglacial (Eemian) hydrographic conditions in the southwestern Baltic Sea based on dinoflagellate cysts from Ristinge Klint, Denmark, Geological Magazine, 144, 987–1013, https://doi.org/10.1017/S0016756807003780, 2007.

Heilmann-Clausen, C. and van Simaeys, S.: Dinoflagellate cysts from the Middle Eocene to ?lowermost Oligocene succession in the Kysing Research Borehole, central Danish Basin, Palynology, 29, 143–204, https://doi.org/10.2113/29.1.143, 2005.

Houben, A. J. P., van Mourik, C. A., Montanari, A., Coccioni, R., and Brinkhuis, H.: The Eocene–Oligocene transition: Changes in sea level, temperature or both?, Palaeogeography, Palaeoclimatology, Palaeoecology, 335–336, 75–83, https://doi.org/10.1016/j.palaeo.2011.04.008, 2012.

Houben, A. J. P., Quaijtaal, W., Wade, B. S., Schouten, S., and Brinkhuis, H.: Quantitative organic-walled dinoflagellate cyst stratigraphy across the Eocene-Oligocene transition in the Gulf of Mexico: A record of climate and sea level change during the onset of Antarctic glaciation, Newsletters on Stratigraphy, 52, 131–154, https://doi.org/10.1127/nos/2018/0455, 2019.

Houben, A., Brinkhuis, H., Iakovleva, A., and Galeotti, S.: Supplement to "Marine palynology of the Alano di Piave Bartonian–Priabonian Global Stratotype Section and Point, NE Italy", Zenodo [data set], https://doi.org/10.5281/zenodo.19338992, 2026.

Iakovleva, A. I.: Organic walled dinoflagellate cyst biostratigraphy of the Bartonian/Priabonian GSSP Alano di Piave section, NE Italy, Review of Palaeobotany and Palynology, 332, https://doi.org/10.1016/j.revpalbo.2024.105233, 2025.

Iakovleva, A. I., Shcherbinina, E. A., Muzylev, N. G., and Aleksandrova, G. N.: Middle–Late Eocene Dinocysts from the Aktumsuk Section (Ustyurt Plateau, Uzbekistan): Biostratigraphy and Paleoenvironments, Stratigraphy and Geological Correlation, 27, 682–706, https://doi.org/10.1134/S0869593819060078, 2019.

Iakovleva, A. I., Waga, D. D., Andreeva-Grigorovich, A. S., and Radionova, E. P.: New palynological data from the middle Eocene deposits of the Kheu reference section (Kabardino-Balkaria, North Caucasus), Stratigraphy and Geological Correlation, 28, 88–106, https://doi.org/10.1134/S0869593820010062, 2020.

Iakovleva, A. I., Zakrevskaya, E. Y., and Shcherbinina, E. A.: Middle Eocene to earliest Oligocene dinoflagellate cysts from southern Armenia: biostratigraphy and palaeoecology, Palynology, 48, https://doi.org/10.1080/01916122.2024.2343902, 2024.

Islam, M. A.: Dinoflagellate cysts from the Eocene of the London and the Hampshire basins, southern England, Palynology, 7, 71–92, 1983.

Jan du Chêne, R. and Châteauneuf, J.-J.: Nouvelles espèces de *Wetzeliella* et *Deflandrea* (Pyrrhophyta, Dinophyceae) de l'Eocène des Alpes occidentales, Revue de Micropaléontologie, 18, 28–37, 1975.

Jenkyns, H. C.: Geochemistry of oceanic anoxic events, Geochemistry, Geophysics, Geosystems, 11, https://doi.org/10.1029/2009GC002788, 2010.

Kaya, M. Y., Brinkhuis, H., Fioroni, C., Atasoy, S. G., Licht, A., Nürnberg, D., and Vural, T.: The Eocene–Oligocene Transition in the Paratethys: boreal water ingression and its paleoceanographic implications, Climate of the Past, 21, 1405–1429, https://doi.org/10.5194/cp-21-1405-2025, 2025.

Klumpp, B.: Beitrag zur Kenntnis der Mikrofossilien des mittleren und oberen Eozän, Palaeontographica, Abteilung A, 103, 377–406, 1953.

Lentin, J. K. and Vozzhennikova, T. F.: The fossil dinoflagellate cysts *Kisselovia* emend. and *Charlesdowniea* gen. nov., Review of Palaeobotany and Palynology, 58, 215–229, https://doi.org/10.1016/0034-6667(89)90087-0, 1989.

Lentin, J. K. and Williams, G. L.: Fossil dinoflagellates: index to genera and species, Geological Survey of Canada, Paper 73-42, 176 pp., 1973.

Lentin, J. K. and Williams, G. L.: A monograph of fossil peridinioid dinoflagellate cysts, Bedford Institute of Oceanography, Report Series, BI-R-75-16, 237 pp., 1976.

Lentin, J. K. and Williams, G. L.: Fossil dinoflagellates: index to genera and species, 1977 edn., Bedford Institute of Oceanography, Report Series, BI-R-77-8, 209 pp., 1977.

Lentin, J. K. and Williams, G. L.: Fossil dinoflagellates: index to genera and species, 1981 edn., Bedford Institute of Oceanography, Report Series, BI-R-81-12, 345 pp., 1981.

Lentin, J. K. and Williams, G. L.: Fossil dinoflagellates: index to genera and species, 1985 edn., Canadian Technical Report of Hydrography and Ocean Sciences, 60, 451 pp., 1985.

Lentin, J. K. and Williams, G. L.: Fossil dinoflagellates: index to genera and species, 1989 edn., American Association of Stratigraphic Palynologists, Contributions Series, 20, 473 pp., 1989.

Liengjarern, M., Costa, L., and Downie, C.: Dinoflagellate cysts from the Upper Eocene-Lower Oligocene of the Isle of Wight, Palaeontology, 23, 475–499, 1980.

Lindemann, E.: Abteilung Peridineae (Dinoflagellatae), in: Die Natürlichen Pflanzenfamilien nebst ihren Gattungen und

wichtigeren Arten insbesondere den Nutzpflanzen, edited by: Engler, A. and Prantl, K., Wilhelm Engelmann, Leipzig, 2, 3–104, 1928.

Lucas-Clark, J. and Helenes, J.: *Ynezidinium*, a new genus within the Gonyaulacaceae (fossil Dinophyceae), J. Micropalaeontol., 19, 113–121, https://doi.org/10.1144/jm.19.2.113, 2000.

Luciani, V., Giusberti, L., Agnini, C., Fornaciari, E., Rio, D., Spofforth, D. J. A., and Pälike, H.: Ecological and evolutionary response of Tethyan planktonic foraminifera to the middle Eocene climatic optimum (MECO) from the Alano section (NE Italy). Palaeogeography, Palaeoclimatology, Palaeoecology, 292, 82–95, https://doi.org/10.1016/j.palaeo.2010.03.029, 2010.

Mann, M. E. and Lees, J. M.: Robust estimation of background noise and signal detection in climatic time series, Climatic Change, 33, 409–445, https://doi.org/10.1007/BF00142586, 1996.

Marret, F. and De Vernal, A.: Dinoflagellate cysts as proxies of environmental, ocean and climate changes in the Atlantic realm during the quaternary, Frontiers in Ecology and Evolution, 12, 1378931, https://doi.org/10.3389/fevo.2024.1378931, 2024.

Menéndez, C. A.: Microplancton fósil de sedimentos Terciarios y Cretácicos del norte de Tierra del Fuego (Argentina), Ameghiniana, 4, 7–15, 1965.

Michoux, D.: Palynostratigraphie de l'Éocène de Montfort-en-Chalosse (Landes, France), Revue de Micropaléontologie, 28, 138–153, 1985.

Morgenroth, P.: Neue in organischer Substanz erhaltene Mikrofossilien des Oligozäns, Neues Jahrbuch für Geologie und Paläontologie, Abhandlungen, 127, 1–12, 1966.

Oreshkina, T. V., Iakovleva, A. I., and Shcherbinina, E. A.: Micropaleontological analysis of Eocene sediments from eastern pre-Caspian region (Borehole no. 57, Shubarsay Mould, Kazachstan), Bulletin of the Moscow Society of Naturalists, Geological Series, 90, 42–80, 2015.

Pascher, A.: Über Flagellaten und Algen, Deutsche Botanische Gesellschaft, Berichte, 32, 136–160, 1914.

Pross, J. and Brinkhuis, H.: Organic-walled dinoflagellate cysts as paleoenvironmental indicators in the Paleogene; a synopsis of concepts, Paläontologische Zeitschrift, 79, 53–59, https://doi.org/10.1007/BF03021753, 2005.

Rossignol, M.: Hystrichosphères du Quaternaire en Méditerranée orientale, dans les sédiments Pléistocènes et les boues marines actuelles, Revue de micropaléontologie, 7, 83–99, 1964.

Sancay, R. H. and Bati, Z.: Late Eocene to Early Oligocene palynostratigraphy of the Western Black Sea, Eastern Paratethys, Turkish Journal of Earth Sciences, 29, 115–138, https://doi.org/10.3906/yer-1905-10, 2020.

Sarjeant, W. A. S.: A restudy of some dinoflagellate cyst holotypes in the University of Kiel Collections. II. The Eocene holotypes of Barbara Klumpp (1953); with a revision of the genus *Cordosphaeridium* Eisenack, 1963, Meyniana, 33, 97–132, 1981.

Schiøler, P.: Dinoflagellate cysts and acritarchs from the Oligocene–Lower Miocene interval of the Alma-1X well, Danish North Sea, Journal of Micropalaeontology, 24, 1–37, https://doi.org/10.1144/jm.24.1.1, 2005.

Shcherbinina, E., Iakovleva, A. I., Gavrilov, Y., Golovanova, O., and Muzylev, N.: Lower Eocene sedimentary succession and microfossil biostratigraphy in the central northern Caucasus basin, Geologica acta: an international earth science journal, 18, 1, https://doi.org/10.1344/GeologicaActa2020.18.1, 2020.

Sluijs, A. and Brinkhuis, H.: High Arctic late Paleocene and early Eocene dinoflagellate cysts, Journal of Micropalaeontology, 43, 441–474, https://doi.org/10.5194/jm-43-441-2024, 2024.

Sluijs, A., Pross, J., and Brinkhuis, H.: From greenhouse to icehouse; organic-walled dinoflagellate cysts as paleoenvironmental indicators in the Paleogene, Earth-Science Reviews, 68, 281–315, https://doi.org/10.1016/j.earscirev.2004.06.001, 2005.

Spofforth, D. J. A., Agnini, C., Pälike, H., Rio, D., Fornaciari, E., Giusberti, L., Kuroda, J., Muttoni, G., and Tescari, C.: Organic carbon burial following the middle Eocene climatic optimum in the central western Tethys, Paleoceanography, 25, https://doi.org/10.1029/2009PA001738, 2010.

Stover, L. E.: Observations on some Australian Eocene dinoflagellates, Geoscience and Man, 11, 35–45, 1975.

Stover, L. E. and Evitt, W. R.: Analyses of pre-Pleistocene organic-walled dinoflagellates, Stanford University Publications, Geological Sciences, 15, 300 pp., 1978.

Stover, L. E. and Hardenbol, J.: Dinoflagellates and depositional sequences in the Lower Oligocene (Rupelian) Boom Clay Formation, Belgium, Bulletin de la Société Belge de Géologie, 102, 5–77, 1994.

Stover, L. E. and Williams, G. L.: A revision of the Paleogene dinoflagellate genera *Areosphaeridium* Eaton 1971 and *Eatonicysta* Stover and Evitt 1978, Micropaleontology, 41, 97–141, 1995.

Streel, M. and Richelot, C.: Wind and water transport and sedimentation of miospores along two rivers subject to major floods and entering the Mediterranean Sea at Calvi (Corsica, France), Grana, 33, 157–164, 1994.

Taylor, F. J. R.: On dinoflagellate evolution, BioSystems, 13, 65–108, 1980.

Toffanin, F., Agnini, C., Fornaciari, E., Rio, D., Giusberti, L., Luciani, V., Reggiani, M., and Pälike, H.: Changes in calcareous nannofossil assemblages during the Middle Eocene Climatic Optimum: Clues from the central-western Tethys (Alano section, NE Italy), Marine Micropaleontology, 81, 22–31, https://doi.org/10.1016/j.marmicro.2011.06.005, 2011.

Van Mourik, C. A., Brinkhuis, H., and Williams, G. L.: Mid-to Late Eocene organic-walled dinoflagellate cysts from ODP Leg 171B, offshore Florida, in: Western North Atlantic Palaeogene and Cretaceous Palaeoceanography, edited by: Kroon, D., Norris, R. D., and Klaus, A., Special Publication – Geological Society of London, 183, 225–251, 2001.

Vasiliyeva, O. N. and Musatov, V. A.: Dinoflagellate cyst and nannoplankton assemblages from the Middle Eocene Kuma Formation of Crimean Peninsula – biostratigraphy and palynofacies, Palaeoworld, 32, 523–546, https://doi.org/10.1016/j.palwor.2022.11.006, 2023.

Vieira, M. and Mahdi, S.: New Paleocene species and biostratigraphic relevance of the genus *Spiniferites* across the North Sea and Norwegian Sea, Review of Palaeobotany and Palynology, 262, 28–43, https://doi.org/10.1016/j.revpalbo.2019.01.002, 2019.

Vieira, M., Mahdi, S., Casas-Gallego, M., and Fenton, J. Three new Paleocene dinoflagellate cysts from the North Sea and the Norwegian Sea, Review of Palaeobotany and Palynology, 258, 256–264, https://doi.org/10.1016/j.revpalbo.2018.09.002, 2018.

Vozzhennikova, T. F.: Iskopaemye peridinei Yurskikh, Melovykh i Paleogenovykh otlozheniy SSSR, Izdatelstvo Nauka, Moscow, 347 pp., 1967.

Wade, B. S., Houben, A. J. P., Quaijtaal, W., Schouten, S., Rosenthal, Y., Miller, K. G., Sluijs, A., Ullgren, J., and Brinkhuis, H.: Multiproxy record of abrupt sea-surface cooling across the Eocene-Oligocene transition in the Gulf of Mexico, Geology, 40, 159–162, https://doi.org/10.1130/G32577.1, 2012.

Wall, D.: Fossil microplankton in deep-sea cores from the Caribbean Sea, Palaeontology, 10, 95–123, 1967.

Westerhold, T., Marwan, N., Drury, A. J., Liebrand, D., Agnini, C., Anagnostou, E., Barnet, J. S. K., Bohaty, S. M., De Vleeschouwer, D., Florindo, F., Frederichs, T., Hodell, D. A., Holbourn, A. E., Kroon, D., Lauretano, V., Littler, K., Lourens, L. J., Lyle, M., Pälike, H., Röhl, U., Tian, J., Wilkens, R. H., Wilson, P. A., and Zachos, J. C.: An astronomically dated record of Earth's climate and its predictability over the last 66 million years, Science, 369, 1383–1387, https://doi.org/10.1126/science.aba6853, 2020.

Williams, G. L.: Palynological biostratigraphy, Deep Sea Drilling Project Sites 367 and 370, Deep Sea Drilling Project, Washington, Initial Reports 41, 783–815, 1978.

Williams, G. L. and Downie, C.: Further dinoflagellate cysts from the London Clay, in: Studies on Mesozoic and Cainozoic dinoflagellate cysts, edited by: Davey, R. J., Downie, C., Sarjeant, W. A. S., and Williams, G. L., British Museum (Natural History) Geology, Bulletin, Supplement 3, 215–236, 1966.

Wilson, G. J.: Some species of *Wetzeliella* Eisenack (Dinophyceae) from New Zealand Eocene and Paleocene strata, New Zealand Journal of Botany, 5, 469–497, 1967.

Wilson, G. J.: Paleocene and Eocene dinoflagellate cysts from Waipawa, Hawkes Bay, New Zealand, New Zealand Geological Survey Paleontological Bulletin, 57, 96 pp., 1988.

Winterer, E. L. and Bosellini, A.: Subsidence and sedimentation on Jurassic passive continental margin, Southern Alps, Italy, AAPG Bulletin, 65, 394–421, 1981.

Zachos, J. C., Dickens, G. R., and Zeebe, R. E.: An early Cenozoic perspective on greenhouse warming and carbon-cycle dynamics, Nature, 451, 279–283, https://doi.org/10.1038/nature06588, 2008.

Zonneveld, K. A. F., Marret, F., Versteegh, G. J. M., Bogus, K., Bonnet, S., Bouimetarhan, I., Crouch, E., de Vernal, A., Elshanawany, R., Edwards, L., Esper, O., Forke, S., Grøsfjeld, K., Henry, M., Holzwarth, U., Kielt, J.-F., Kim, S.-Y., Ladouceur, S., Ledu, D., Chen, L., Limoges, A., Londeix, L., Lu, S.-H., Mahmoud, M. S., Marino, G., Matsuoka, K., Matthiessen, J., Mildenhal, D. C., Mudie, P., Hanh, L., Parris, P. J., Radi, T., Rochon, A., Sangiorgi, F., van der Schootbrugge, B., Solignac, S., Turon, J.-L., Verleye, T., Wang, Y., Wang, Z., and Young, M.: Atlas of modern dinoflagellate cyst distribution based on 2405 data points, Review of Palaeobotany and Palynology, 191, 1–197, https://doi.org/10.1016/j.revpalbo.2012.08.003, 2013.